Small-scale testing of micromechanical response of cemented carbides

A dissertation submitted to partial fulfilment of the requirements for the degree of Doctor of Philosophy by

Daniela Andreina Sandoval Ravotti

Department of Materials Science and Metallurgical Engineering
Doctorate program in Materials Science and Engineering
Universitat Politècnica de Catalunya - BarcelonaTech

Advisors: Prof. Luis Miguel Llanes Pitarch
Prof. Joan Josep Roa Rovira

UNIVERSITAT POLITÈCNICA DE CATALUNYA
BARCELONATECH
Departament de Ciència dels Materials i Enginyeria Metal·lúrgica

Thesis presented by compendium of publications
Barcelona, Spain
September 2019

1 µm

Cover photo:

Micropillar of 2 μm in diameter milled by means of Focused Ion Beam (FIB) on the surface sample of a WC-CoNi cemented carbide, with 10 wt.% of binder and a WC mean grain size of around 1 μm.

"Todos tenemos adentro una insospechada reserva de fortaleza que emerge cuando la vida nos pone a prueba"

—Isabel Allende, La isla bajo el mar

A ti, Tierra de colores y sabores
A ti, Venezuela

PREFACE

This dissertation is the result of the research work conducted by the author to obtain the degree of Doctor of Philosophy in Materials Science and Engineering at the Universitat Politècnica de Catalunya-BarcelonaTech (UPC). This work was conducted between February 2016 and September 2019 under the supervision of Professors Luis Miguel Llanes Pitarch and Joan Josep Roa Rovira. Experimental work was carried out within the Centre d'Integritat Estructural i Fiabilitat dels Materials (CIEFMA) group from the Department of Materials Science and Metallurgical Engineering (CMEM) of the UPC, and the Agenzia Nazionale per le Nuove Tecnologie, l'Energia e lo Sviluppo Economico Sostenibile (ENEA). The presented work is original, unless otherwise detailed references are provided.

This PhD thesis is submitted as compendium of scientific publications and it is structured in six chapters. In *Chapter 1*, an introduction to cemented carbides is given, together with an overview on the criticality of W and Co as main raw materials for this composite material, and a state of the art on nano- and micromechanical testing techniques available nowadays. In *Chapter 2* the objectives of this work are presented. *Chapter 3* describes in depth the experimental details and techniques used in this thesis to achieve the goals proposed in *Chapter 2*. Scientific publications derived from the research work carried during this PhD thesis are presented in *Chapter 4*. Results are summarized in *Chapter 5*. Finally, general conclusion and perspectives are presented in *Chapter 6*.

—Daniela Sandoval

ABSTRACT

Cemented carbides - also referred to as hardmetals - are composite materials widely used in different industry fields within applications involving wear such as cutting, machining and drilling, among others, due to their outstanding wear resistance. The most commonly cemented carbides used are WC-Co grades, due to cobalt (Co) wettability of tungsten carbide (WC), and adhesion characteristics. Emergence of new applications, the existence of advanced characterization techniques, economic and environmental aspects, among others, encourages the development of a new cemented carbides generation containing other binding phases as nickel (Ni) and iron (Fe) or alloys of them. Furthermore, Co powder has been classified as very toxic for the human health and the combination carbide-cobalt hardmetals dust has shown to be even more toxic than both pure Co and W.

The success of substitution of the main constituents of cemented carbides, have been commonly measured in terms of their final mechanical properties at macroscale such as hardness, Palmqvist fracture toughness and transverse rupture strength (TRS); and their structural integrity under service-like conditions, such as corrosion resistance, thermal shock and fatigue resistance, etc. In this sense, general framework of the effect of their microstructural characteristics – carbide mean grain size, volume fraction and chemical nature of constitutive phases – on the mechanical response is well established at the macroscale. However, assessment of the individual role of binder and carbide phases in cemented carbides at local scale i.e. microscale, is yet to be studied in depth.

Within micromechanical testing, special attention has being paid to the micropillar compression approach because its advantages: the stress-state is nominally uniaxial, allowing a straight conversion of the measured load-displacement data into flow curves; sample preparation by means of Focused Ion Beam (FIB) milling is a relatively easy machining route; it involves the use of a conventional nanoindenter with a flat-end tip; and, it can be performed ex-situ or in-situ by using Scanning Electron Microscopy (SEM) or Transmission Electron Microscopy (TEM) techniques. However, attention have to be paid to sample sizes since it has been well established that intrinsic properties of crystalline materials such as yield stress and strength, can be greatly influenced by extrinsic factors such as volume. For instance, results have evidenced an inverse relation between hardness and the indentation depth at the micro- and nanometric length scales. Regarding cemented carbides, recent studies showed that changes in volume fraction of binder and carbides in samples can lead to wide scatter in results of Young's modulus measured at the microscale.

Following the above ideas, in this PhD thesis uniaxial compression of micropillars and nanoindentation have been selected to *evaluate the role of binder and carbides regarding their chemical*

nature and microstructural dimensions, i.e. carbide mean grain size and binder mean free path, in the mechanical properties of cemented carbides and their mechanical response at local scales.

This thesis is presented by a compendium of scientific publications in which several specific objectives are studied individually. The first publication aims to evaluate the effect of the micropillar diameter on the micromechanical response of WC-Co. In the second publication, the effect of WC mean grain size and volume fraction of both carbide and binder phases are investigated. Results allowed to *overcome the size effect issue – usually found when testing in the micro- or nanometer regime – by selecting an appropriate sample size, to accomplish reliability on the mechanical properties evaluated at local length scales.*

Third and fourth publications are devoted to investigating the mechanical properties of cemented carbides with partial or total substitution of WC or Co as main constitutive phases. In this sense, in the third publication nanoindentation is used to *evaluate the intrinsic hardness of constitutive phases and flow stress of the constrained binder* in a WC-(W,Ti,Ta,Nb)C-Co cemented carbide. Finally, in the fourth paper three materials, one with Co and two with partial and total substitution of Co as binder, respectively, were studied to *investigate the influence of the chemical nature of the binder on the overall mechanical response of cemented carbides, on the basis of plastic deformation phenomena and failure mechanisms induced by uniaxial compression of micropillars*.

The outcomes derived from the research carried out during this PhD thesis evidence that small scale testing of complex composite materials such as cemented carbides by means of uniaxial compression of micropillars and nanoindentation techniques, allows to evaluate the role of each constitutive phase on their mechanical properties and response. In doing so, an appropriate sample size should be selected, in order to obtain reliable results of the overall behavior of the material.

RESUMEN

Los carburos cementados – también llamados metales duros – son materiales compuestos ampliamente utilizados en diferentes áreas industriales, en aplicaciones que involucran desgaste como corte, mecanizado y taladrado, entre otras, debido a su sobresaliente resistencia al mismo. Los carburos cementados más comúnmente usados son grados WC-Co, debido a la mojabilidad y adhesión que tiene el cobalto (Co) sobre el carburo de tungsteno (WC). El surgimiento de nuevas aplicaciones, la existencia de técnicas avanzadas de caracterización, aspectos económicos y ambientales, entre otros, motivan el desarrollo de una nueva generación de carburos cementados que contengan otras fases ligantes como níquel (Ni) y hierro (Fe) o aleaciones de ellos. Además, el polvo de Co ha sido clasificado como muy tóxico para la salud humana y la combinación de metales duro carburo-cobalto, ha demostrado ser más tóxica que Co o W puros.

En éxito en la substitución de los componentes principales de los carburos cementados, ha sido comúnmente medido basado en sus propiedades mecánicas finales, evaluadas a escala macrométrica, como dureza, tenacidad de la fractura Palmqvist y resistencia a rotura; y también en su integridad estructural al ser sometidos a condiciones de servicio, como resistencia a la corrosión, choque térmico, fatiga, etc. En este sentido, la visión general del efecto de sus características microestructurales – tamaño medio de carburo y fracción volumétrica y naturaleza química de sus fases constitutivas – en la respuesta mecánica de carburos cementados está bien establecida a escala macrométrica. Sin embargo, el efecto individual de ambas fases ligante y carburo, en el compuesto a escala local, es decir, escala micrométrica, aún debe ser estudiado en profundidad.

En el ámbito de ensayos micromecánicos, se ha prestado especial atención a la compresión de micropilares debido a sus ventajas: el estado de tensión es nominalmente uniaxial, lo que permite una conversión directa de los datos medidos de carga-desplazamiento en curvas de flujo; la preparación de la muestra mediante el fresado con haz de iones focalizados (FIB por sus siglas en inglés) es una ruta de mecanizado relativamente fácil; implica el uso de un nanoindentador convencional con punta plana; y, puede realizarse *ex situ* o *in situ* utilizando técnicas de microscopía electrónica de barrido (SEM por sus siglas en inglés) o microscopía electrónica de transmisión (TEM por sus siglas en inglés). Sin embargo, se debe prestar atención al tamaño de la muestra, ya que se ha establecido que las propiedades intrínsecas de los materiales cristalinos, como el límite elástico y la resistencia, pueden verse influidas por factores extrínsecos como el volumen. Por ejemplo, los resultados han evidenciado una relación inversa entre la dureza y la profundidad de indentación en escalas de longitud micro- y nanométrica. Con respecto a los carburos cementados, estudios recientes mostraron que los cambios en la fracción de volumen de ligante

y carburos en las muestras pueden conducir a una amplia dispersión en los resultados del módulo de Young medido a microescala.

Siguiendo las ideas anteriores, en esta tesis doctoral se han seleccionado la compresión uniaxial de micropilares y la nanoindentación como técnicas experimentales para *evaluar el papel del ligante y los carburos con respecto a su naturaleza química y dimensiones microestructurales, es decir, el tamaño medio del grano del carburo y el camino libre medio del aglutinante, en las propiedades mecánicas de carburos cementados y su respuesta mecánica a escala local*.

Esta tesis doctoral es presentada como un compendio de publicaciones científicas en el que una serie de objetivos específicos se estudian individualmente. La primera publicación tiene como objetivo evaluar el efecto del diámetro del micropilar en la respuesta micromecánica de WC-Co. En la segunda publicación, se investiga el efecto del tamaño medio de grano WC y la fracción de volumen de las fases de carburo y ligante. Los resultados permitieron *superar el problema del efecto del tamaño de la muestra – generalmente presente al realizar ensayos en el régimen micro- o nanométrico – mediante la selección de un tamaño de muestra apropiado para lograr fiabilidad en las propiedades mecánicas evaluadas en escalas de longitud pequeñas*.

Las publicaciones tercera y cuarta se dedican a investigar las propiedades mecánicas de los carburos cementados con sustitución parcial o total de WC o Co como fases constitutivas principales. En este sentido, en la tercera publicación, la nanoindentación se utiliza para *evaluar la dureza intrínseca de las fases constitutivas y el esfuerzo de fluencia del ligante constreñido*, en un carburo cementado WC-(W,Ti,Ta,Nb)C-Co. Finalmente, en el cuarto artículo científico, se estudiaron tres materiales, uno con Co y dos con substitución parcial y total de Co, respectivamente, para *investigar la influencia de la naturaleza química del ligante en la respuesta mecánica general de los carburos cementados, basado en fenómenos de deformación plástica y mecanismos de falla inducidos por la compresión uniaxial de micropilares.*

Los resultados derivados de la investigación llevada a cabo durante esta tesis doctoral demuestran que las pruebas a pequeña escala de materiales compuestos complejos – como los carburos cementados – mediante compresión uniaxial de micropilares y nanoindentación, permiten evaluar el papel de cada fase constitutiva en su respuesta y propiedades mecánicas. Al hacerlo, se debe seleccionar un tamaño de muestra apropiado para obtener resultados confiables del comportamiento general del material.

RESUM

Els carburs cimentats – també coneguts com a metalls durs – són materials compostos àmpliament usats a diversos camps industrials en aplicacions que comporten desgast, com en eines de tall, mecanitzat o trepat, a causa de la seva excepcional resistència al mateix. Els carburs cimentats més comunament usats són graus de WC-Co, per les característiques d'humectabilitat de cobalt (Co) amb el carbur de tungstè (WC) i la seva adhesió. L'aparició de noves aplicacions, l'existència de tècniques de caracterització avançades, aspectes econòmics i ambientals, entre d'altres, fomenta a el desenvolupament d'una nova generació de carburs cimentats que continguin altres fases d'unió com níquel (Ni) i ferro (Fe) o els seus aliatges. A més, la pols de Co ha estat classificada com a molt tòxica per a la salut humana i la combinació de pols de metall dur carbur-cobalt ha demostrat ser encara més tòxica que el Co o el W purs.

L'èxit de la substitució dels constituents principals dels carburs cimentats es mesura habitualment en termes de propietats mecàniques finals, com la duresa, la tenacitat de fractura Palmqvist i la resistència a fractura transversal (TRS) a escala macroscòpica; i en termes d'integritat estructural en condicions similars a servei, com ara la resistència a corrosió, resistència a xocs tèrmics i fatiga, etc. En aquest sentit, el marc general dels efectes de les característiques microestructurals – mida mitjana dels carburs i fracció de volum i naturalesa química de les fases constitutives – en la resposta mecànica dels carburs cimentats està ben establerta en l'escala macroscòpica. No obstant això, encara cal estudiar en profunditat el paper individual de la fase lligant i dels carburs en l'escala local, és a dir, a l'escala micromètrica.

Pel que fa als assajos micromecànics, s'ha prestat especial atenció a la compressió de micropilars gràcies als seus avantatges: l'estat de tensions és nominalment uniaxial, permetent una conversió directa de les mesures càrrega-desplaçament a corbes de flux; la preparació de mostres mitjançant un microscopi de feix de ions (FIB) és una tècnica de mecanitzat relativament senzilla; implica l'ús d'un nanoindentador convencional amb una punta plana; i es pot realitzar ex-situ o in-situ mitjançant un microscopi electrònic de rastreig (SEM) o de transmissió (TEM). Tot i això, cal parar atenció a les dimensions de les mostres, ja que està ben establert que les propietats intrínseques dels materials cristal·lins, com ara la tensió i la resistència, poden estar molt influïdes per factors extrínsecs com ara el volum. Per exemple, els resultats han evidenciat una relació inversa entre la duresa i la profunditat d'indentació a les escales micro- i nanomètriques. Respecte als carburs cimentats, estudis recents han demostrat que canvis en la fracció volumètrica de lligant i carburs comporta una àmplia dispersió en els resultats de mòdul de Young mesurat a la microescala.

Seguint aquestes idees, en aquesta tesi doctoral s'ha seleccionat la compressió uniaxial de micropilars i nanoindentació per *avaluar el paper del lligant i els carburs respecte la seva naturalesa química i dimensions microestructurals, és a dir, grandària mitjana del carbur i camí lliure mig del lligant, en les propietats mecàniques dels carburs cimentats i la seva resposta mecànica a escales locals.*

Aquesta tesi es presenta com a compendi de publicacions científiques en les quals s'estudien objectius específics individualment. La primera publicació té com a objectiu avaluar l'efecte del diàmetre del micropilar en la resposta micromecànica del WC-Co. A la segona publicació, s'investiguen l'efecte de la mitja mitjana del gra de WC i la fracció de volum de les fases de carbur i lligant. Els resultats han permès *superar el problema de l'efecte de mida – habitual quan s'assaja a escales micro- i nanomètrica – seleccionant una mida de mostra adequada per tal d'aconseguir propietats mecàniques fiables avaluades a escales locals.*

La tercera i quarta publicacions estan dedicades a investigar les propietats mecàniques dels carburs cimentats amb substitució parcial o total de WC o Co com a fase constitutiva principal. En aquest sentit, en la tercera publicació s'usa la tècnica de nanoindentació per *avaluar la duresa intrínseca de les fases constitutives i la tensió de fluxe del lligant constret* en un carbur cimentat WC-(W,Ti,Ta,Nb)C-Co. Finalment, en el quart treball s'han estudiat tres materials, un amb Co i dos amb substitució parcial o total de Co com a lligant, respectivament, per tal d'investigar la influència de la naturalesa química del lligant en la resposta mecànica global dels carburs cimentats, segons fenòmens de deformació plàstica i mecanismes de fallada induïts per compressió uniaxial de micropilars.

Els resultats derivats de la investigació realitzada durant aquesta tesi doctoral demostren que els assajos a escala petita de materials compostos complexos com ara els carburs cementats mitjançant compressió uniaxial de micropilars i tècniques de nanoindentació permeten avaluar el rol de cada fase constitutiva en les propietats i resposta mecàniques. Per fer-ho, cal seleccionar una mida de mostra adequada per tal d'obtenir resultats fiables del comportament global del material.

List of publications

This PhD dissertation is presented as a compendium of articles listed below. Impact factor (IF) and quartile (Q) are included.

ARTICLE I

D.A. Sandoval, A. Rinaldi, J.M. Tarragó, J.J. Roa, J. Fair, L. Llanes. Scale effect in mechanical characterization of WC-Co composites. Int. J. Refract. Metals Hard Mater. 72, 157-162 (2018). https://doi.org/10.1016/j.ijrmhm.2017.12.029. IF: 2.606. Q1 (11/75) in Metallurgy & Metallurgical Engineering. Q2 (101/285) in Materials Science Multidisciplinary.

ARTICLE II

D.A. Sandoval, A. Rinaldi, A. Notargiacomo, O. Ther, E. Tarrés, J.J. Roa, L. Llanes. Influence of specimen size and microstructure on uniaxial compression of WC-Co micropillars. Ceram. Int. 45, 15934-15941 (2019). https://doi.org/10.1016/j.ceramint.2019.05.102. IF: 3.057. Q1 (43/158) in Materials Science, Ceramics.

ARTICLE III

D.A. Sandoval, J.J. Roa, O. Ther, E. Tarrés, L. Llanes. Micromechanical properties of WC-(W,Ti,Ta,Nb)C-Co composites. J. Alloys Compd. 777, 593-601 (2019). https://doi.org/10.1016/j.jallcom.2018.11.001. IF: 3.779. Q1 (62/285) in Materials Science Multidisciplinary. Q1 (4/75) in Metallurgy & Metallurgical Engineering.

ARTICLE IV

D.A. Sandoval, A. Rinaldi, A. Notargiacomo, O. Ther, J.J. Roa, L. Llanes. WC-base cemented carbides with partial and total substitution of Co as binder: Evaluation of mechanical response by means of uniaxial compression of micropillars. Int. J. Refract. Metals Hard Mater. 84, 105027 (2019). https://doi.org/10.1016/j.ijrmhm.2019.105027. IF: 2.606. Q1 (11/75) in Metallurgy & Metallurgical Engineering. Q2 (101/285) in Materials Science Multidisciplinary.

Other contributions

Non-included related articles

S. Fang, R. Lima, **D.A. Sandoval**, D. Bähre and L. Llanes. Ablation investigation of cemented carbides using short-pulse laser beams. Proc. CIRP. 68 172-177 (2018). doi: https://doi.org/10.1016/j.procir.2017.12.042.

J.J. Roa, E. Jiménez-Piqué, J.M. Tarragó, **D.A. Sandoval**, A. Mateo, J. Fair, L. Llanes. Hall-Petch strengthening of the constrained metallic binder in WC-Co cemented carbides: Experimental assessment by means of massive nanoindentation and statistical analysis. Mater. Sci. Eng. A. 676 487-491 (2016). http://dx.doi.org/10.1016/j.msea.2016.09.020.

Poster and oral presentations

Oral and poster contributions at international conferences

D.A. Sandoval, A. Rinaldi, A. Notargiacomo, O. Ther, J.J. Roa, L. Llanes. Deformation of WC-based cemented carbides with partial and total substitution of Co as binder by means of uniaxial compression of micropillars. 11th International Conference on the Science of Hard Materials. Oral contribution (Khao Lak, Thailand, 25th – 29th March 2019).

J.J.Roa, E.Jiménez-Piqué, J.M.Tarragó, D.A. Sandoval, H. Besharatloo, A. Mateo, L. Llanes. Small-Scale mechanical response of cemented carbides. 5th International Conference on Powder Metallurgy in Asia. Keynote contribution by J.J.Roa (Pune, India, 19th – 21th February 2019).

D.A. Sandoval, J.J. Roa, O. Ther, E. Tarrés, L. Llanes. Fracture behavior and fatigue life of WC-NiMo cemented carbides. EuroPM 2018 Congress and Exhibition. Oral contribution (Bilbao, Spain, 14th – 18th October 2018).

D.A. Sandoval, A. Rinaldi, O. Ther, J.J. Roa, L. Llanes. Small scale testing of WC-Co by means of uniaxial compression of micropillars. Workshop on micromechanical properties of hard materials. Oral contribution (Barcelona, Spain, 27th – 29th June 2018).

D.A. Sandoval, J.M. Tarragó, A. Rinaldi, A. Notargiacomo, J.J. Roa, J. Fair, L. Llanes. Influence of the mean carbide size on the micromechanical response of WC-Co hardmetals. EuroPM 2017 Congress and Exhibition. Oral contribution (Milano, Italy, 1st – 5th October 2017).

D.A. Sandoval, J.J.Roa, J. Fair, L.Llanes. Scale effect in mechanical characterization of WC-Co composites. 19 Plansee Seminar. Poster exhibition (Reutte, Austria, 29th May – 2nd June 2017).

J.J.Roa, E.Jiménez-Piqué, D.A. Sandoval, J.M.Tarragó, J. Fair, E.Tarres, L.Llanes. Small scale mechanical response of WC-Co cemented carbides. 19 Plansee Seminar. Oral contribution by E.Jiménez-Piqué (Reutte, Austria, 29th May – 2nd June 2017).

D.A. Sandoval, J.J.Roa, J. Fair, E.Tarres, L.Llanes. Micromechanical properties of WC(Ti,Ta,W)C-Co composites: Hardness anisotropy and flow stress determination for the constrained metallic binder. International Materials Research Meeting in the Greater Region “Current Trends in the Characterisation

of Materials and Surface Modification". Oral contribution by J.J.Roa (Saarbrücken, Germany, 6th – 7th April 2017).

D.A. Sandoval, J.J. Roa, J. Fair, L. Llanes. Small scale mechanical response of W(Ti,Ta)C-Co Composites. EPMA World PM2016 Congress & Exhibition. Oral contribution by J.J. Roa (Hamburg, Germany, 9th – 13th October 2016).

Oral and poster contributions at national conferences

D.A. Sandoval, S. Gordon, S. Abouelaz, O. Ther, E. Tarrés, J.J. Roa, L. Llanes. Fracture and fatigue behavior of WC-NiMo cemented carbides. VII Congreso Español de Pulvimetalurgia y II Congreso Iberoamericano de Pulvimetalurgia. Poster exhibition by L. Llanes (Madrid, Spain, 24th – 26th June 2019).

D.A. Sandoval, O. Ther, J.J. Roa, L. Llanes. Fracture behavior of WC-NiMo composites. V Congreso Hispano-Luso de Cerámica y Vidrio. Oral contribution (Barcelona, Spain, 8th – 10th October 2018).

L.Llanes, J.M.Tarragó, D. Coureaux, E.Tarrés, G.Farga, D.A. Sandoval, J.J. Roa, E.Jiménez-Piqué. Damage tolerance of cemented carbides: key parameter for improving mechanical reliability. V Congreso Hispano-Luso de Cerámica y Vidrio. Plenary contribution by L.Llanes (Barcelona, Spain, 8th – 10th October 2018).

D.A. Sandoval, J.J. Roa, J. Cugnoni, J. Fair, E. Tarrés, L. Llanes. Prediction of the macroscopic behavior of WC-(Ti,Ta,W)C-Co from the intrinsic micromechanical properties of its constitutive phases. VI Congreso Nacional de Pulvimetalurgia y I Congreso Iberoamericano de Pulvimetalurgia. Oral contribution (Ciudad Real, Spain, 7th – 9th June 2017).

D.A. Sandoval, J.J. Roa, J. Fair, L. Llanes. Evaluación de las propiedades micromecánicas de compuestos de W(Ti,Ta)C-Co. XIV Congreso Nacional de Materiales. Oral contribution (Gijón, Spain, 8th – 10th June 2016).

Table of contents

List of figures

Figure 3.6. Nanoindentation system mounted in a SEM holder: a) detail of motion station and location of samples; and b) detail of nanoindentation system and nanoindentation tip.

Figure 3.6. Nanoindentation system mounted in a SEM holder: a) detail of motion station and location of samples; and b) detail of nanoindentation system and nanoindentation tip.

List of tables

Glossary of symbols and abbreviations

Glossary of symbols

μ_i	Arithmetic mean value of hardness
a	Indentation radius
a, c	Lattice parameters
A_o	Area of micropillars 1 μm
$C_{carbide}$	Contiguity of the carbide phase
D	Characteristic microstructural length scale
d_b	Diameter of the micropillar at the bottom
$d_{carbide}$	WC mean grain size
d_{pillar}	Micropillars diameter
d_t	Diameter of the micropillar at the top
E	Elastic Modulus
E_b	Young's modulus of the bulk
E_i	Young's modulus of diamond tip
fcc	Face centered cubic
F_{meas}	Measured force
h	Displacement
H	Hardness
h^*	Characteristic length
hcp	Hexagonal closed packed
h_i	Depth of indentation
H_o	Hardness in the limit of infinite depth
HV	Vickers Hardness
L	Characteristic size
L_o	Initial length of micropillars
L_I	Linear intercept
l_{pillar}	Micropillars length
N	Constant = 0.45
N_i	Number of indentations
$N_{WC/Binder}$	Number of carbide/cobalt intercepted interfaces
$N_{WC/WC}$	Number of carbide/carbide intercepted interfaces
P	Load
p_i	Mechanical properties
Ra	Average roughness
TRS	Transverse Rupture Strength
$V^{wt}{}_{binder}$	Binder content in weight percent
V_{binder}	Volume fraction of binder
V_{Co}	Volume fraction of Co
vol.%	Volume percent
V_{WC}	Volume fraction of WC
wt.%	Weight percent
$X_{sneddon}$	Displacement corrected by the Sneddon's approach
α	Taper angle
α	Stress

ε	Strain
λ_{binder}	Binder's mean free path
ν_b	Poisson's ratio of the bulk
ν_i	Poisson's ratio of diamond
ρ_c	Experimental density of the composite
ρ_{WC}	Density of WC
σ_{flow}	Flow stress of the binder phase
σ_i	Standard deviation of the mechanical property pi
ψ	Constraint factor of the binder phase

Glossary of abbreviations

AM	Additive manufacturing
APT	Ammonium paratungstate
CCD	Charge couple device
CDF	Cumulative distribution function
CRMs	Critical Raw Materials
CSM	Continuous Stiffness Module
CVD	Chemical vapor deposition
EBSD	Electron Backscattered Diffraction
ECCI	Electron Channeling Contrast Imaging
FESEM	Field Emission Scanning Electron Microscope/Microscopy
FIB	Focused Ion Beam
GHS	Globally Harmonized System of Classification and Labelling of Chemicals
HIP	Hot Isostatic Pressing
HSS	High speed steel
ISE	Indentation Size Effect
PVD	Physical vapor deposition
REV	Representative Elementary Volume
SEM	Scanning Electron Microscope/Microscopy
SPM	Scanning Probe Microscopy
STEM	Scanning Transmission Electron Microscopy
TEM	Transmission Electron Microscopy

Chapter 1

Introduction

1 Introduction

1.1. Cemented carbides - History and status

Cemented carbides - also referred to as hardmetals - are a group of composite materials that show outstanding mechanical properties such as hardness and fracture toughness, and excellent wear resistance. Such combination of properties makes cemented carbides suitable to produce structural and tool materials capable of working under stringent requirements. The microstructure of cemented carbides is heterogeneous, and it is constituted by hard but brittle carbides phase bond by one soft and tough metallic binder. The first ones are refractory carbides of the transition metals (WC, TiC, TaC, Cr_3C_2 or Mo_2C), and the last one is a metal from the iron group, more often cobalt (Co) or nickel (Ni) and their alloys [1].

Refractory carbides of transition metals from the groups IV, V and VI show an interstitial structure that combines metallic, covalent and ionic bonds, being the group of materials with a high melting point. They also exhibit high hardness and strength with high thermal and chemical stability [2]. On the other hand, the metallic binder phase is a ductile and softer phase that contributes to improve the toughness of cemented carbides [1]. The unique combination of hardness and toughness given by its constitutive phases - in comparison with other hard materials – position cemented carbides as the most versatile materials used mainly in the tooling, mining, and oil and gas industries [3].

Development of cemented carbides started during World War I in Germany due to the need to replace diamond drawing dies for a less expensive material, in the production of tungsten (W) filaments [1,4]. Several attempts were made without success, until 1923, when tungsten carbide (WC) with added Ni was sintered. With time, Ni was changed by Co, obtaining a good ceramic-metal combination, suitable to produce fine W wires of good quality [4,5].

The new material was commercialized in 1926 under the name “WIDIA” (from German terminology “wie Diamant” - meaning like diamond). In 1927 tools made with WIDIA were shown to the international public for the first time at the Spring Fair of Leipzig [5]. From this point on, the production of cemented carbides along with the born of new companies started to grow simultaneously. High speed steel (HSS) used in cutting tools production started to be replaced by cemented carbides: cutting speeds were increased due to the improvement in wear resistance at high temperature of cemented carbides, extending lifetime of tools [5].

Between 1929 and 1935, Schwarzkopf, Comstock and McKenna alloyed tungsten carbide with titanium carbide (TiC), molybdenum (Mo_2) and titanium carbide (TaC), improving the potential of WC-Co as tool for high speed machining. Ever since, the improvement of the properties and performance of cemented carbides have been continuous [6]. A summarized chronology of the development of cemented tungsten carbides during the XX century is presented in Table 1.1.

Table 1.1. Development of cemented carbides industry during the XX century [5–7].

Year	***Event***
1923-25	First WC-Co tool
1929-31	Development of WC-TiC-Co and WC-TaC(VC, NbC)-Co grades
1938	WC-Cr_3C_2-Co
1948-70	Sub-micron WC-Co hardmetals
1965-75	Hot isostatic pressing (HIP)
1965-78	TiC, TiN, Ti(C,N), HfC, HfN and Al_2O_3 CVD coatings on WC-based hardmetal
1969-71	Thermochemical surface hardening
1974-77	Polycrystalline diamond on WC-based hardmetal
1973-78	Multi-carbide, carbonitride/nitride and multiple carbide/carbonitride/nitride/oxide coatings
1981	Many thin coatings with AION (aluminum oxynitride) layers
1983-92	Sinter-HIP
1992-95	Plasma CVD diamond coating
1993-95	Coating complex carbonitrides
1994	Nanocrystalline cemented carbides

In the last 30 years, the production of cemented carbides has grown rapidly. From a total annual production of around 20,000 tons in 1993, to nearly 60,000 tons in the year 2008. The accelerated growth was a consequence of the entry of China into the cemented carbides market. Only in China, the production has raised from 7000 tons in the year 2001 to 28,000 tons in 2017 [8]. The fast growth of production of cemented carbides in particular for metal cutting has driven improvements in Chemical Vapor Deposition (CVD) coated cemented carbides with Co-enriched surface zone [9]. Moreover, the demand on submicron grained grades is increasing due to a trend on miniaturized electronic devices (in particular computers and phones), and to improvements in Physical Vapor Deposition (PVD) techniques which have widened the use of PVD coated metal cutting inserts [10]. Compared to other hard materials, cemented carbides represent 50% of the total world market with almost 65% of the total production related to metal cutting tools.

Opportunities to improve cemented carbides include tailoring their microstructure by substitution and/or alloying of both carbide and binder phases, and other processing routes as additive manufacturing (AM) for which recent investments have reached nearly one billion US dollars, nearly half of it being devoted to the medical industry [11].

1.2. Structure of cemented carbides

In cemented carbides, the most commonly used ceramic phase is tungsten carbide (WC) [12], while the metallic binder is often cobalt (Co), followed by nickel (Ni) and iron (Fe) in order of importance [13]. The binder is selected for its wettability with the carbide and adhesion characteristics. In this regard, Co shows outstanding wetting of WC, resulting in full densification and finally higher values of toughness when comparing with other metallic binders [14]. Furthermore, Ni is found to be the best binder for hardmetals based on TaC [1,15]. An improvement on wettability and adhesion of the carbide phase can be achieved by alloying the known binders. Addition of chromium (Cr) to Co or Ni tends to reduce toughness at room temperature but improves strength and hot hardness at high temperatures [1].

1.2.1. Ceramic carbides

More than 98% of cemented carbides grades contain WC. Besides WC, tungsten can also form the sub carbide W_2C and cubic sub-stoichiometric γ-WC_{1-x}. The range of homogeneity of WC in the W-C phase diagram is small, 50 at.% or 6.13 wt.% [1]. Although tungsten monocarbide is the principal hard phase found in cemented carbides, a deficit on carbon content in WC-Co may promote any of the other carbide phases as shown in Figure 1.1 [16].

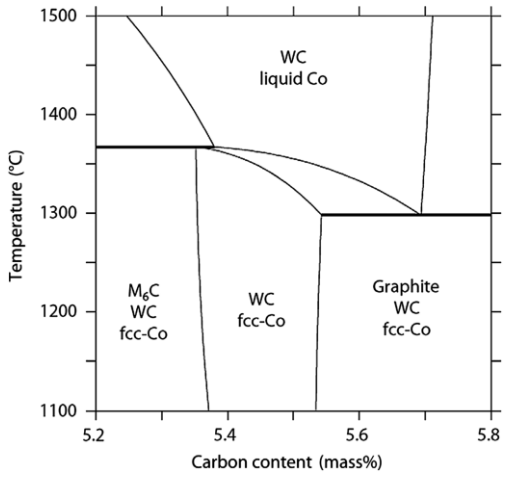

Figure 1.1. Section of the W-C-Co phase diagram of a WC-Co cemented carbide with 10 wt.%Co [16]. Image from [17].

WC particles exhibit a hexagonal close packed (hcp) crystal structure with lattice parameters $a = 0.2906\ nm$ and $c = 0.2837\ nm$, with a ratio $c/a = 0.976$. WC crystals grown from liquid-metal solutions exhibit the shape shown in Figure 1.2 a, which is also the shape of WC grains in cemented carbides as seen in Figure 1.2 b. The shape adopted by WC in cemented carbides owes to the high polarity of the prismatic crystal planes of $(10\bar{1}0)$ type due to the different spacing of the W and C planes of [1010] directions; therefore, there are two sets of equivalent $(10\bar{1}0)$ planes, instead of six ones [1]. Because of its

non-centrosymmetric structure of WC, the microhardness is strongly anisotropic, i.e. hardness of the basal plane (0001), the prismatic plane ($10\bar{1}0$) and intermediate orientations are different [1].

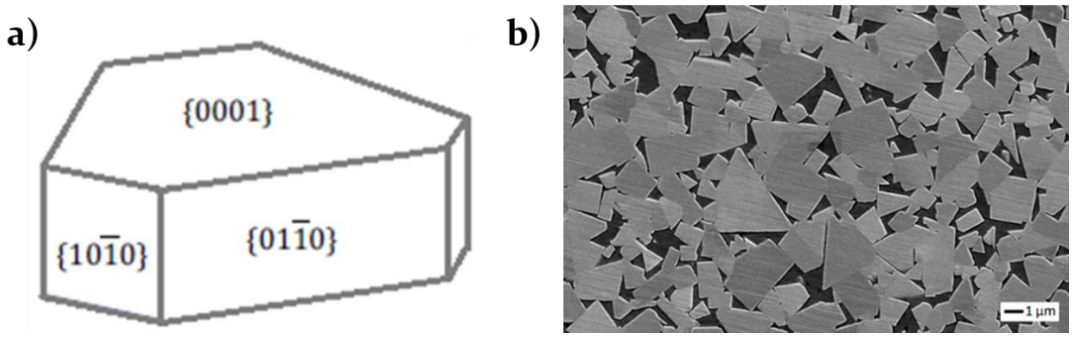

Figure 1.2 a) Schematic representation of truncated WC grains shape in WC-Co composites [18], and b) a typical microstructure of WC-Co cemented carbides. The light and dark phases correspond to the carbide and to the metallic binder, respectively.

Despite the existence of other carbides with higher hardness than WC, extremely high Young's modulus (around 700 GPa) and high thermal conductivity (1.2 J cm^{-1} s^{-1} K^{-1}) of WC are advantageous properties for cutting applications [1]. In WC-Co alloys, WC shows appreciably plastic deformation during compression test due to the mechanical behavior of the metallic binder [1].

TiC, ZrC, HfC, VC, NbC and TaC carbides are also used to produce hardmetals. These carbides are face centered cubic (fcc), melt congruently and exhibit higher hardness than WC. Especially, TiC and TaC are used as reinforcement particles in cemented carbides [1]. However, they have limited toughness; thus, they are more brittle than WC [1]. During production of WC-Co hardmetals, TiC is added to improve resistance to chemical diffusion that cause cratering in cutting tools [19], and to reduce electrical conductivity for some applications [3]. On the other hand, TaC is added to cutting tool grades because it has higher fracture toughness than TiC [19]. Addition of TiC, TaC and/or NbC enhances corrosion resistance of WC-Co grades [3].

Some properties of WC and cubic carbides are summarized in Table 1.2.

Table 1.2. Properties of cubic refractory carbides commonly used for hardmetals production [1,15,19].

Material	*Young's Modulus (GPa)*	*Vickers Hardness (HV50)*	*Density (g cm^{-3})*	*Melting temperature (°C)*
WC	*696*	*13-22*	*15.70*	*2800**
TiC	450	30	4.94	3100*
TaC	285	18	14.50	3800
Cr_3C_2	373	14	6.66	1800*
Mo_2C	533	15	9.78	2500
NbC	388	20	7.80	3600
VC	422	29	5.71	2700

(*) Dissociation temperatures.

1.2.2. Metallic binder

Cobalt is the most commonly used material as metallic binder in cemented carbides. Pure Co shows an allotropic transformation from an hcp structure up to around 415 °C to a cubic structure (fcc) at higher temperatures [15]. The prevalence of one form or another may affect the mechanical properties of the composite material [1]. Stability of the two allotropic phases is also affected by grain size: their structures favor the cubic form [12]. In sintered WC-Co alloys, Co shows a cubic lattice because stabilization of it by dissolved W and C, and cannot be transformed by annealing [1,12]. The stabilization of the fcc structure of Co is influenced by the W and C content dissolved as solid solution inside the metallic Co binder, ranging from 0.5-2 at.% (0.1-0.4 wt.%) and 0-5.9 at.% (0-17 wt.%) respectively [20].

1.3. Critical raw materials

In 2010, European Union (EU) launched a list of 14 raw materials considered critical based on economic importance and the risk of supply disruption. The list was updated to 20 in 2014 (see Figure 1.3) [21]. These materials are considered non-energy raw materials and reduced access to them may depress construction, automotive, aerospace and tool industries which are vital industrial sector in EU economy [22]. In this sense, European partnerships have arisen since 2013, to act towards ensuring a sustainable supply of raw materials to the European economy, including actions on the extraction, processing, recycling and substitution of critical raw materials (CRMs) [23]. However, implementation of these actions is not straight-forward. It implies great efforts from the industrial, technological and research communities to obtain reliable substitute materials with comparable or improved performances, easily and quickly integrable in the production processes, potentially recyclable and with lower risk to the environment and human health [22].

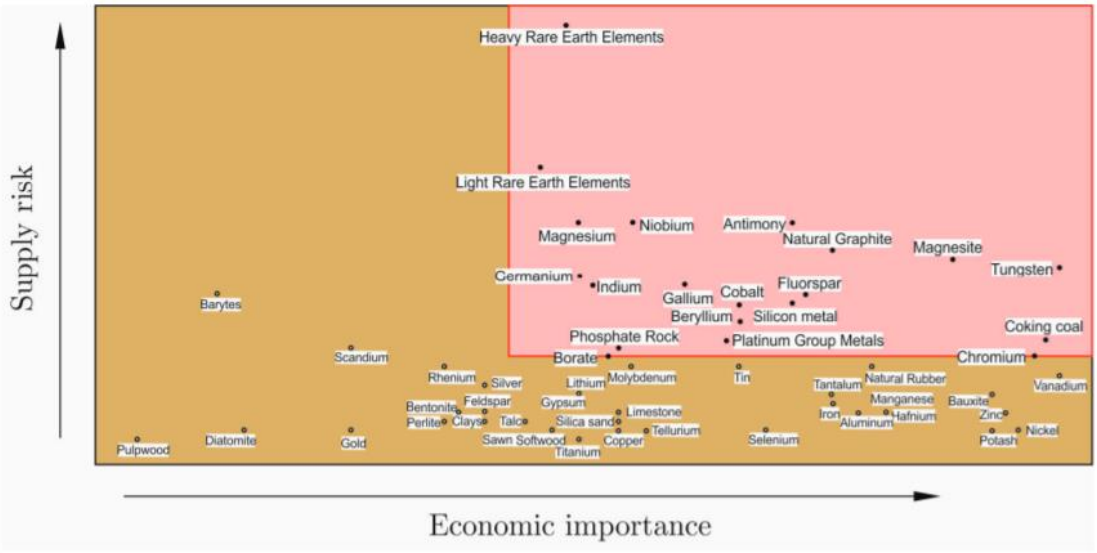

Figure 1.3. Supply risk vs. Economic importance for EU of elements. Upper right corner (red color) frames those elements with high supply risk and of high economic importance for EU (critical raw materials) [22].

Regarding cemented carbides, as it has been referred above, Co is the most commonly used metal binder [1]. Meanwhile, W exhibits high melting point among other metallic elements and its monocarbide (WC) finds the largest application in cemented carbides due to its high hardness, low density and elevated corrosion resistance [2]. Around 12% of the consumed Co is in hardmetals [24] and almost half of the total Co in the world is located in Democratic Republic of Congo. On the other hand, the world's largest deposits of W are placed in China, followed by Canada, Russia, USA, Australia, Korea, Turkey, Bolivia and others. Location of tungsten makes it hardly accessible to the "industrial world" [25]. By 2015, the tungsten consumption in China was around 47000 tons/year (59% of the total world consumption) [10]. Difficult access to CRMs impacts directly in their prices. Important fluctuations of prices of raw materials can be seen in Figure 1.4.

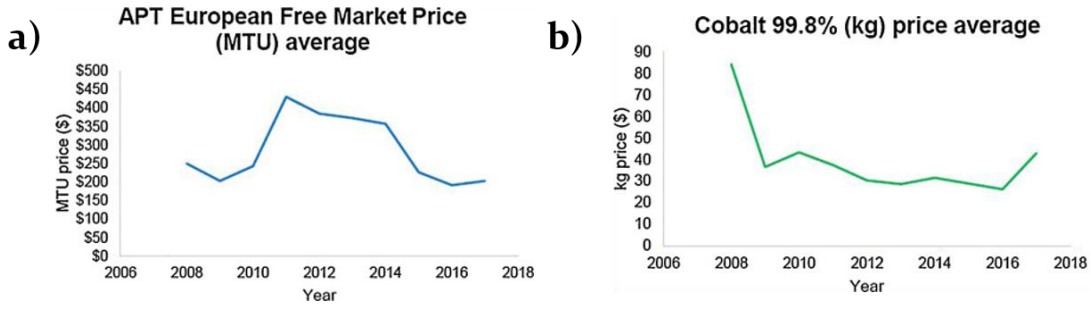

Figure 1.4. Global price of a) ammonium paratungstate (APT), and b) cobalt per metric ton units (MTU). Data from January 2019. Source: Metal bulletin.

Moreover, Co powder has been classified as very toxic for the human health and the combination carbide-cobalt hardmetals dust has shown to be even more toxic than both pure Co and W [26,27]. On

the other hand, WO_3 "suspected for causing cancer" by the Globally Harmonized System of Classification and Labelling of Chemicals (GHS) [25], forms at the surface of WC by oxidation and chemical reactions with metal working fluids, and release to the environment through wear particles [28].

1.3.1. Substitution of W and Co in WC-Co cemented carbides

Since few decades ago, investigations have been devoted to develop new composites with partial or total substitution of Co by more economic and less toxic materials, with equal or improved properties and simpler production techniques as to increase the efficiency of recycling process [7,10,25].

Vasel *et al.* [29] progressively substituted Co with Ni in a WC-Co hardmetal and reported that addition of Ni retarded the martensitic transformation of Co fcc to hcp. Martensitic transformation was proven to be the main work-hardening mechanism of Co [30]. Thus, addition of Ni shifted the predominant deformation mechanism from martensitic transformation to slip and twinning, decreasing hardness as the Ni content increased [29]. The progressive replacement of Co by Ni also leads to a decrease in ultimate compressive strength [31]. However, partial or complete replacement of Co by Ni does not alter transverse rupture strength (TRS) values [31].

A comparison of the mechanical properties made by Human *et al.* [32] for several binder alloys of Ni-Mo, Ni-Cr-Mo with pure Ni and Co, revealed that hardness, Palmqvist fracture toughness and TRS of Ni alloys were comparable with those of Co. However, both hardness and toughness were affected by the binder and content of alloying elements. More recently, Tarragó *et al.* [33,34] reported higher fracture toughness and lower hardness, for WC-CoNi than for WC-Co cemented carbides with similar binder mean free paths. As Cr and Mo increased, hardness increased but toughness decreased given its role as grain growth inhibitors. While severe increase in grain growth occurred with plain Ni binder, rising Cr and Mo resulted in a finer microstructure; thus, higher hardness and lower toughness. Hardness of WC-Ni can be raised with moderate additions of Cr_3C_2 and further additions improves TRS. However, very high contents of Cr in WC-10Co-4Cr was found to lower TRS [32].

Even though mechanical properties can slightly differ for cemented carbides with binder alloys as Ni-Cr-Mo, in comparison with cemented carbides with Co binder, selection of other binders can be done to improve other properties such as corrosion resistance. For instance, substitution of Co by Ni-Cr and Ni-Cr-Mo binders promotes an increase in corrosion resistance of hardmetals [32]. Both WC-Co and WC-Ni are corrosion resistant in solutions above pH 7. However, WC-Ni is better than WC-Co in acidic solutions and even more when adding Cr. Furthermore, addition of Mo enhance the pitting resistance in chloride environments [35].

Elevated corrosion resistance can be also obtained by adding TiC [35] or by replacing 40% of WC with TaC [36]. Higher hardness and lower density of TiC, together with its great availability in regions accessible to the industrial world, have made it the most studied carbide to replace WC. The use of TiC remains in cutting tools given its hardness and good wear resistance. Although brittleness and poor hot-deformation, compared to WC, holds back the use in other applications [37].

1.4. Microstructural parameters of cemented carbides

Both mechanical and tribological performance of cemented carbides are related to the chemical nature, amount and size of carbide and binder phases [15]. The common parameters used to characterize the microstructure of hardmetals are the mean grain size of the carbide particles ($d_{carbide}$) and the volume content of binder (vol.%). Correlation of both is done by contiguity of the carbide phase ($C_{carbide}$) and binder's mean free path (λ_{binder}) [1,6,38]. The mentioned microstructural parameters are illustrated in Figure 1.5.

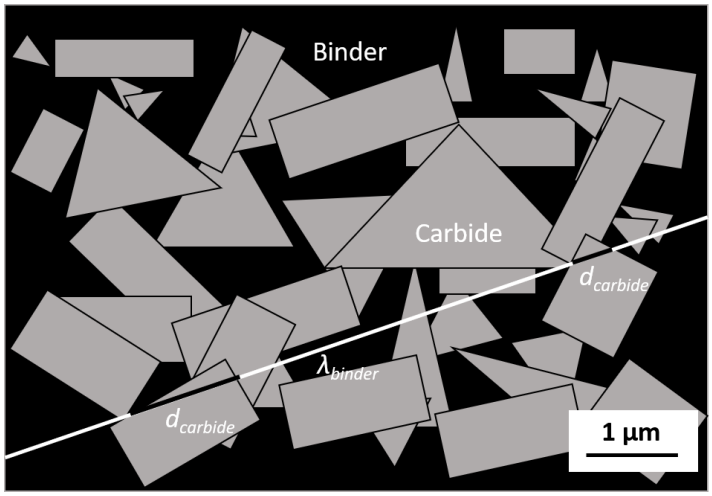

Figure 1.5. Microstructural parameters commonly determined for cemented carbides. In the image, black and light phases correspond to binder and ceramic particles, respectively.

1.4.1. Mean grain size of carbide phase

Mean grain size is a statistical concept that refers to the average size of the carbide particles that constitute a cemented carbide. The final mean grain size and the size distribution depends on the grain size of the starting powders, the milling and sintering conditions and the composition of the binder [5], e.g. addition of small amounts of VC or TaC to WC-Co leads to grain size refinement while high C contents promote the growth of WC grains [19]. Mean grain size of carbide phase can range from less than 0.5 µm to more than 50 µm, as seen in Figure 1.6 [39].

The mean grain size of the carbide phase is related to the final properties of the cemented carbide. Alloys with smaller grain mean size are harder. On the other hand, the larger the WC grains, the wider the metallic binder layer between the hard grains; and thus, the higher the fracture toughness of the alloy [40,41].

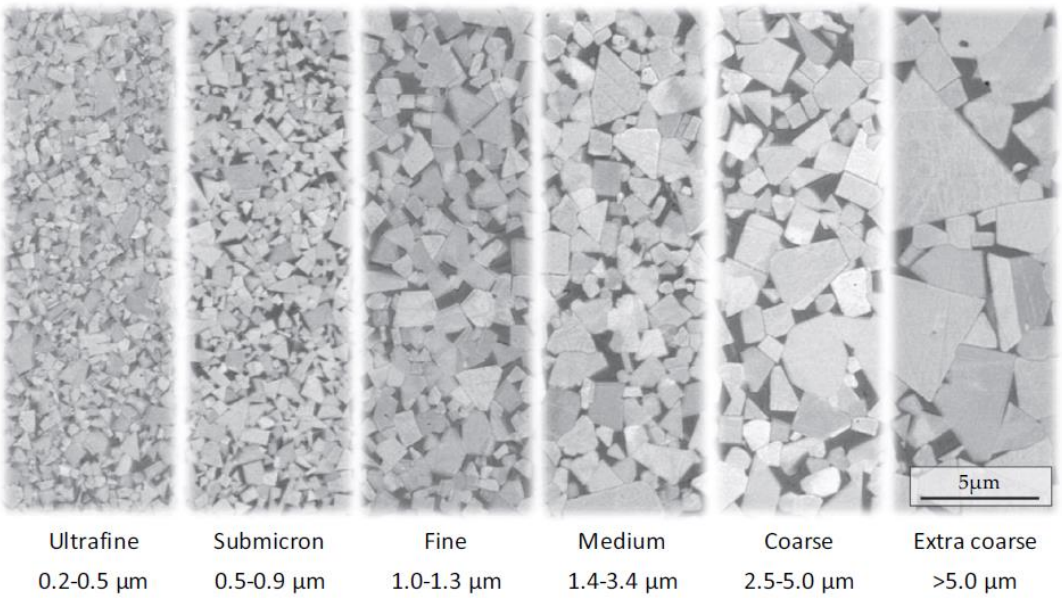

Figure 1.6. Classification of cemented carbides according to the mean grain size of the carbide phase [39].

The most commonly used method to determine the carbide grain size is the linear interception (LI) method. It consists in measuring the length of the carbides crossed by a line in a scanning electron microscope (SEM) micrograph [42]. More recently, given the production of nano-grained and ultrafine grades of hardmetals, it becomes harder to detect smaller grains in a SEM micrograph. Automatic grain-size analysis where the shape of the particle (circularity) is used to calculate mean size of WC particles have been proposed, e.g. [43–45].

1.4.2. Binder content

The binder content has a relevant influence on the mechanical properties of cemented carbides. It is usually given in weight percentage (wt.%), but the use of the volume percentage (vol.%) or the volume fraction (V_{binder}) can be a more informative value [38]. Conversion of wt.% to V_{binder} can be done by applying the following expression:

$$V_{binder} = \frac{1+\frac{1-V_{binder}^{wt}}{V_{binder}^{wt}\rho_{WC}}(\rho_{WC}-\rho_{c})}{1+\frac{1-V_{binder}^{wt}}{V_{binder}^{wt}}} \qquad \text{Equation 1}$$

where V_{binder} is the binder content in volume, $V^{wt}{}_{binder}$ is the binder content in weight percent, ρ_{WC} is the density of tungsten carbide (15.65 g/cm³), and ρ_c is the experimental density of the composite.

In cemented carbides, the state of aggregation of the carbide phase varies not only due to the processing history but also with the binder content. It then ranges from isolated carbide particles dispersed in the binder to a highly connected skeleton of contiguous carbide particles, for high binder content to low binder content respectively [19].

1.4.3. Contiguity

The contiguity partially describes the state of aggregation of the carbide phase. It is defined as the measure of the extent of the carbide grain boundary area relative to the total surface area of the carbide grains [19]. The following expression is used to calculate contiguity of cemented carbides:

$$C_{WC} = \frac{2N_{WC/WC}}{2N_{WC/WC}+N_{WC/Binder}} \quad \text{Equation 2}$$

where $N_{WC/WC}$ and $N_{WC/Binder}$ are the number of carbide/carbide and carbide/cobalt intercepted interfaces [38].

With increasing sintering time, the contiguity decreases possibly due to a grain agglomeration and boundary migration, or to continuous Co penetration of WC/WC grain boundaries [19].

Values of contiguity for a fixed volumetric content of binder are extremely scattered. It is attributed for some authors to the possible effect of grain size distribution of carbide phase, suggesting that for larger grain size, the larger the contiguity of the carbide phase [38,46]. However, some authors suggest the independence of the contiguity on the grain size. In this case it should be expressed as a function of the binder content exclusively [47]. Other authors report that grain shapes also have an influence in contiguity [48].

Roebuck and Almond [38] expressed the contiguity as a function of the binder content for WC-Co alloys. They stated that for each value of volume fraction of Cobalt (V_{Co}) there is a wide range of $C_{Carbide}$ values due to grain size and distribution. However, they reported an expression to determine C for $0.35>V_{Co}>0.05$ as follows:

$$C_{Carbide}(V_{Co})^n = D \quad \text{Equation 3}$$

where *n* and *D* are constants with 0.45 and 0.2 values, respectively.

More recently, Coureaux [49] proposed an empirical equation to determine contiguity as a function of V_{binder} and d_{WC} for fine and medium grades of cemented carbides. Afterwards, Tarragó *et al.* [45] improved and extended it for determination of contiguity for ultrafine and nanometric cemented carbides (Equation 4).

$$C_{Carbide} = 0.036 + 0.9733 * e^{\frac{-d_{WC}}{3.90825}} * e^{\frac{-V_{binder}}{0.24913}} \quad \text{Equation 4}$$

1.4.4. Mean free path

The mean free path, also called the mean linear intercept in the binder phase (λ_{binder}), is used to describe the distribution of the binder phase in cemented carbides. It is the most important parameter to characterize the geometry of the binder phase, due to its inverse relation with the specific surface of the binder phase (carbide/binder interface per unit volume of binder) [1]. This microstructural characteristic, along with contiguity and volume content of binder, constitute the primary structural parameters of cemented carbides. They are interrelated, as proposed by Lee and Gurland [46], according to Equation 5, even for varying binder phase content and sintering conditions.

$$\lambda_{binder} = \frac{1}{1-C_{Carbide}} \frac{V_{binder}}{V_{WC}} d_{WC} \quad \text{Equation 5}$$

where V_{WC} is the volume fraction of WC.

The λ_{binder} increases when rising the carbide mean grain size and/or the volume fraction of binder. An increase in λ_{binder} results in a higher fracture toughness of the composite; thus, lower hardness [38].

1.5. Mechanical testing at micro- and nanometric length scales

Micro and nano-mechanical testing have their origins in nanoindentation [50] and scanning probe microscopy (SPM) [51], applied to surfaces of materials and coatings and to the mechanics of nano-objects, respectively [52]. An important advance in the era of micromechanics came with the invention of micro-compression of micropillars milled by using a focused ion beam (FIB) in Ni single crystals, and subsequently deformed with a nanoindenter equipped with a flat punch [53]. A scheme of the micro- and nano-testing techniques available nowadays is shown in Figure 1.7.

Initially, mechanical testing at small length scales targeted understanding of size effects in single crystals. In this sense, it became very well understood that when the sample volume is greatly reduced, intrinsic mechanical properties of materials (e.g. yield stress ad strength) may exhibit an extrinsic behavior. This in known as size-scale effect and it can be defined as a change in material properties – mechanical, electrical, optical, or magnetic – due to a change in dimensions of internal structure or the dimensions of the sample [53].

For many years it was a fact that the strength of a bulk material is strongly dependent of the characteristic length scale of its microstructure, i.e. grain or precipitate size, twin boundary spacing, or dislocation density. Thus, this intrinsic size governs the mechanical properties and post-elastic deformation at all samples dimensions [54]. However, increasing experimental activities on small-scale samples has shown that at micron and sub-micron scales, this is no longer true. For example, for single crystals of metallic structures, it has been shown that the ultimate tensile strength and the yield strength scale with external sample size following a power law, i.e. they exhibit the now more common phenomenon “smaller is stronger” [54–57].

Micromechanical testing field have evolved into studying the influence of microstructure in the plastic response of materials with a second phase [58], such as inclusions [59–62], grain boundaries [63–68], and interfaces [69–74], as well as fracture [75–81]. Furthermore, not only micro- and nano-mechanical testing have been used for mechanical testing of materials with dimensions from a few atoms up to the micrometer scale (including particles, sheets and thin films, etc.), to qualitatively determine their mechanical properties, but also for bulk materials to enhance their performance based on the knowledge that mechanical failure starts locally with formation and accumulation of defects that finally lead to fracture [58].

In this thesis, a combination of nanoindentation, micropillar compression and imaging techniques such as SEM, transmission electron microscopy (TEM) and electron backscattered diffraction (EBSD) were selected to evaluate the mechanical response of cemented carbides at small length scales.

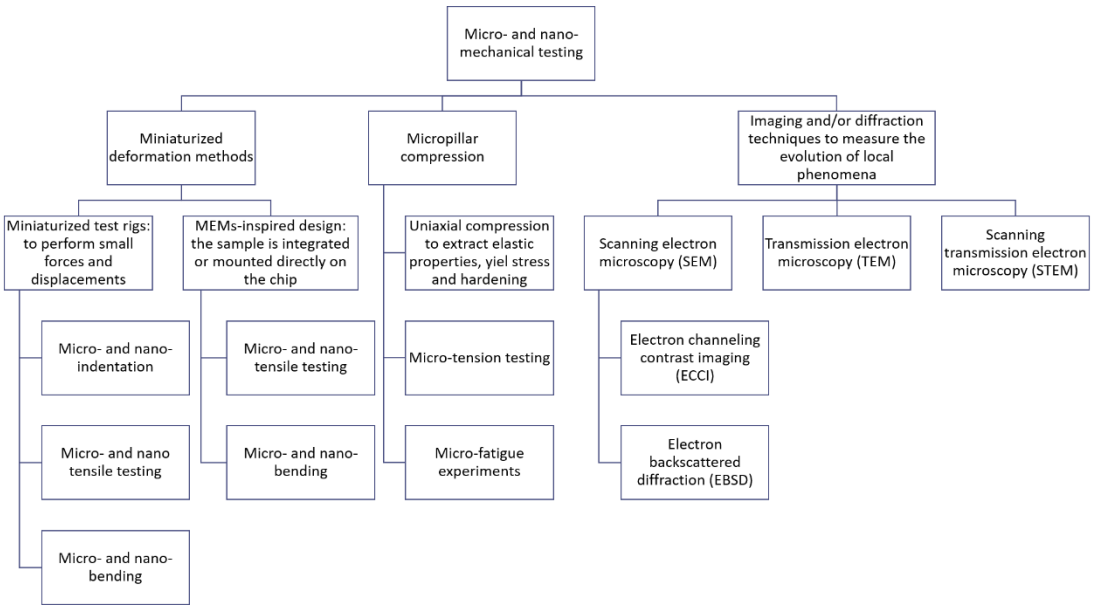

Figure 1.7. Scheme of the current available techniques for micro- and nano-mechanical testing [58].

1.6. Mechanical properties and response of cemented carbides

Cemented carbides are key materials in the group of heterogeneous composite group with mainly a hard phase and a soft one. WC-Co combination is a successful example of the optimal implementation of microstructural design towards enhanced performance and reliability in extremely demanding applications (e.g. Refs. [1,17,38]).

Hardness is among the key parameters for most of the applications in which cemented carbides are involved: machining tools, mining and drilling, drawing, forging, stamping, etc. Understanding of microstructure-hardness relationship, from theoretical, analytical and experimental viewpoints, have been a matter of study since decades ago (e.g. Refs. [46,82–85]). However, intrinsic response of constitutive phases is usually not considered in the overall behavior of the composite material. For example, it has been stablished that hardness of WC is anisotropic [86–93]. Furthermore, binder is a Co-W-C alloy in which the amount of the alloying elements plays an important role on the intrinsic hardness and deformation mechanisms [1,94], while disposition of the surrounding carbide particles, i.e. constraint degree, affects its flow stress in the composite [95].

Structure of cemented carbides is given by a carbide skeleton, reinforced by a ductile metallic phase interconnected trough the composite. Effective toughening of the material comes in one hand, from the deformation of ductile ligaments of binder [96–99]. On the other hand, high toughness of cemented carbides have been associated with effective interaction between the intrinsic residual stresses – mostly thermal residual stresses from cooling after sintering – and the external applied stresses [100–104]. At macroscopic scale, plasticity of cemented carbides is the result of multiple plasticity mechanisms

occurring in each constitutive phase at the microscale. Thus, performance of cemented carbides is directly dependent upon the intrinsic response of both carbides and constrained binder.

Regarding the above, consideration of the local response of each constitutive phase would allow better analytical and modelling outcomes from the viewpoint of microstructural design of metal-reinforced ceramic-based composites.

1.7. Mechanical properties and response of cemented carbides at local length scales

General framework of microstructural effects on the mechanical response of cemented carbides is well established at the macroscale (e.g. Refs. [1,33,38,83,84,105,106]). However, mechanical response of both binder and carbide phases, as well as assessment of the individual role of the binder phase in cemented carbides at local scale i.e. at the microscale, is yet to be studied in depth. Regarding small scales, many studies have found estimated data in satisfactory agreement with experimental data by assuming an effect by the length scale, such as a Hall-Petch relationship in intrinsic hardness of constitutive phases, independently from the constrain factors [46,106–110].

Within this context, nanoindentation and micropillar compression approach can give insights on the local response of cemented carbides, not only in terms of mechanical properties (hardness, stress and strain), but also in terms of the role played by its constitutive phases. In this sense, recent studies have been devoted to evaluate the mechanical response of WC particles at small length scales [111], as well as that of the composite material [95,112–115].

1.7.1. Uniaxial compression of micropillars

Micro-compression testing has become a commonly used technique to study the mechanical response of various materials in the micrometer and sub-micrometer regime [116–120] especially due to the simplicity of converting measured load (P)-displacement (h) data into flow curves, given that stress-state is nominally uniaxial [121].

Other advantages of micropillar compression may be mentioned. First, the absence of important strain gradients that can mask the effect of the volume alone and free surfaces due to the appearance of important extrinsic contributions [122]. Second, sample preparation and testing are relatively simple by using Focused Ion Beam (FIB), which is the most commonly used technique to mill micropillars.

Some limitations of this approach are related to the micropillar taper angle; the confinement of the pillar at the base of the specimen, imposed by the surrounding material; and misalignment between

the micropillar and the punch [123]. All of them can lead to non-uniformity of the micropillar stress state, underestimation of the elastic modulus, and possible buckling instead of compression, among others [55,121].

Given the strong influence of the specimen size in the mechanical response, most of the recent investigations have been advocated to fully describe and understand the size effect in strength and plasticity by means of micropillar compression, e.g. [57,124–126]. To the best knowledge of the author, no studies of this nature have been carried on cemented carbides. Csanádi *et al.* [111] compressed micropillars milled in basal and prismatic oriented grains of WC in a WC-Co cemented carbide, to study the influence of the orientation of WC in their mechanical response. More recently, Tarragó *et al.* [114] deepened in the mechanical deformation and failure of ceramic-metal composite by compressing micropillars of a WC-Co composite with 15 wt.% of Co. They revealed that carbide-carbide and carbide-binder interfaces are preferential sites for irreversible deformation and failure phenomena. Furthermore, plasticity phenomena were found preferentially in the binder phase close to the WC/Co interfaces where maximum triaxiality stress conditions prevail.

Actual interest in using cemented carbides in tools and components ranging from the decimeter to the nanometer sizes requires a deep understanding of its mechanical behavior at small scales, including the effect of the specimen size. In this regard, further investigation should be done not only to evaluate the mechanical response at small length scales, but also to stablish the influence of the microstructural parameters in the mechanical response of small specimens.

1.7.2. Hardness measured at small length scales

Macro- and microindentation tests are not well suited to determine the micromechanical properties of individual constitutive phases in cemented carbides, due to the small sizes of binder's means free path and mean carbide grain size usually found in hardmetals. For these materials nanoindentation is a more appropriate technique to determine mechanical properties such as hardness and elastic modulus for their constitutive phases.

Compared with traditional hardness testing, nanoindentation allows to evaluate mechanical response of individual phases heterogeneously distributed in the bulk material. Among its advantages, it is possible to set penetration depth and/or maximum load in the equipment; the elastic modulus can be directly determined from test data; specimen volume can be in the order of tens of microns; and the mechanical properties can be determined without the need to visualize the residual imprint [127]. However, some disadvantages can be mentioned such as the need of a good surface finish in order to

avoid errors in determination of the contact point due to high roughness; errors in measurements due to thermal drift; and errors in hardness and elastic modulus values, due to the rounding effect of the nanoindenter tip [128].

Hardness (H) and elastic modulus (E) are the most commonly measured properties as a function of the displacement into surface, determined due to the presence of the continuous stiffness module (CSM) in the equipment. This allows reliable determination of both properties at the same time [129], directly extracting them from the loading-unloading or load-displacement (P-h) curves [128].

Indentation size effect

Hardness values calculated at different applied loads, from mN to N or from the macro to nano-scale, are completely different. At low applied loads i.e. low penetration depths, hardness values are higher than those obtained at higher loads; this phenomenon is known as indentation size effect (ISE) [127]. It is caused by possible combination of several mechanisms as strain gradients effects, roughness of specimen surface, irregularities of the deformed volume, and activation of different mechanisms in the elastic/plastic deformation regime [127].

Nix and Gao [130] proposed the following relation to determine accurately the hardness (H) without any ISE effect:

$$\frac{H}{H_0} = \sqrt{1 + \frac{h^*}{h_i}} \qquad \text{Equation 6}$$

where H is the hardness for a given depth of indentation h_i, H_o is the hardness in the limit of infinite depth, and h^* is a characteristic length that depends on the shape of the indenter.

Indentation length scale

Determination of an intrinsic mechanical properties of the materials comprising a given representative elementary volume (REV) can be done by indentation data acquired by considering a critical indentation depth to avoid significant length scale effect [131].

By fixing indentation depth and grid size, the imprint and the plastic field inside each phase are confined [113]. A good approximation is proposed by Constantinides *et al.* [131] where REV and characteristic size (L) must obey the length scale separability condition (Equation 7), where (h, a) are the indentation depth and indentation radius, D is a characteristic microstructural length scale, and d is

the characteristic size of the largest microstructural or mechanical heterogeneity contained in the REV. A good estimate according to Ref. [131] is that D is of the order of 3 times the penetration depth for Berkovich indentation.

$$d \ll L \ll (h, a, D) \qquad \text{Equation 7}$$

Chapter 2

Aims and scope

2 Aims and scope

Given the nature of hardmetals they are mostly used in strategic industrial sectors such as aerospace, oil and gas, tool industry, among others. With the current need to substitute Co and WC by alternative binders and carbides that outcome the severe working conditions, comes the need to understand the role of each constitutive phase in the overall mechanical response of the composite. In this sense, mechanical testing at small length scales arises as a suitable approach to study mechanical response, deformation phenomena, and mechanisms of failure, localized at interest points along the composite constitution.

Following the above ideas, the main objective of the present project is *to evaluate the role of the chemical nature of their constitutive phases and microstructural features, i.e. mean WC grain size and binder mean free path, in the mechanical properties and response of cemented carbides evaluated at the micro- and nanometric length scales*. For this purpose, uniaxial compression of micropillars and nanoindentation were found appropriate. Accordingly, several specific objectives are aimed:

- Study of the sample size effect, i.e. micropillar diameter, on the micromechanical response of WC-Co, to accomplish reliability on the mechanical properties evaluated at small length scales.

- Assessment of the influence of mean WC grain size and volume fraction of constitutive phases within micropillars, on the mechanical properties of W-Co determined by means of uniaxial compression of micropillars.

- Evaluation of the intrinsic hardness of constitutive phases and flow stress for the constrained Co binder, of a Co-base cemented carbide with partial substitution of WC by the mixed (W,Ti,Ta,Nb)C cubic carbide, and its influence on the overall mechanical response of the composite.

- Investigation of the influence of binder's chemical nature on the plastic deformation phenomena and failure mechanisms induced by uniaxial compression in WC-base cemented carbides with partial and total substitution of Co as binder.

Chapter 3

Experimental aspects

3 Experimental aspects

3.1. Materials and sample preparation

The main purpose of this PhD thesis is to determine the mechanical properties of cemented carbides at small length scales. The studied materials are in the scope of interest of Hyperion Materials & Technologies, who kindly provided them for the investigation. One of the main goals of the work is to determine the influence of microstructural parameters such as carbide mean size and binder mean free path, as well as of chemical nature of the binder in the mechanical behavior of cemented carbides. In doing so, three WC-Co cemented carbide grades with different WC mean grain sizes and two additional grades with partial and total substitution of Co as binder (WC-CoNi and WC-NiMo) were selected. Binder content of all the studied grades was selected to be similar, between 10 and 11 wt.%.

Table 3.1 summarizes the proposed grades of cemented carbides to be evaluated in the present PhD thesis. There, the "Grade" column indicates the name used for each alloy according to the following order: **binder content** (in number)/**binder's chemical nature.** WC mean grain size is classified in the "GS" column as: fine (F), medium (M) and coarse (C).

Table 3.1. Composition and microstructural aspects for cemented carbide grades selected for the present study.

Grade	GS	Binder	Additives	wt.% Binder	d_{WC} (μm)	C_{WC}	λ_{binder} (μm)
WC-Co	F	Co	Cr_3C_2	10	0.4 ± 0.2	0.5 ± 0.1	0.2 ± 0.1
WC-Co	M	Co	Cr_3C_2	11	1.1 ± 0.7	0.4 ± 0.1	0.4 ± 0.3
WC-Co	C	Co		10	2.3 ± 1.4	0.3 ± 0.1	0.7 ± 0.5
WC-CoNi	M	CoNi		8 Co – 2 Ni	1.0 ± 0.8	0.4 ± 0.1	0.4 ± 0.3
WC-NiMo	M	NiMo	Cr_3C_2	9 Ni – 1 Mo	1.0 ± 0.8	0.4 ± 0.1	0.4 ± 0.3
WC-(W,Ti,Ta,Nb)C-Co	M	Co		11	0.8 ± 0.2	0.5 ± 0.1	0.4 ± 0.2

A good surface finish is mandatory to obtain reliable measurements of microstructural parameters, as well as results from micromechanical testing. Before polishing, samples were cut and mounted. The polishing was done according to standard ASTM E3-01 [132] in a semiautomatic polisher following the steps shown in Table 3.2. The las step with colloidal silica was repeated several times to obtain an average roughness *Ra* below 0.3 μm. After polishing, the samples were cleaned in acetone within an ultrasonic bath for 30 min.

Table 3.2. Polishing steps for surface sample preparation.

Step	Time (min)	Disc/Cloth	Speed (rpm)	Force (N)
1	5	MD Piano 120	150	15
2	5	MD Piano 220	150	15
3	5	MD Piano 500	150	15
4	10	MD Piano 1200	150	15
5	20	Diamond paste 30 µm	150	15
6	15	Diamond paste 6 µm	150	15
7	5	Diamond paste 6 µm	150	10
8	30	Diamond paste 3 µm	100	15
9	10	Colloidal silica	50	10

Mean WC grain size was determined by following LI method according to standard ISO4499 [42] with six SEM micrographs (Figure 3.1), acquired with a SEM Jeol JSM-7001F unit. Two-phase parameters, C_{WC} and λ_{binder}, were estimated from best-fit empirical equations given in the literature [38,45,49].

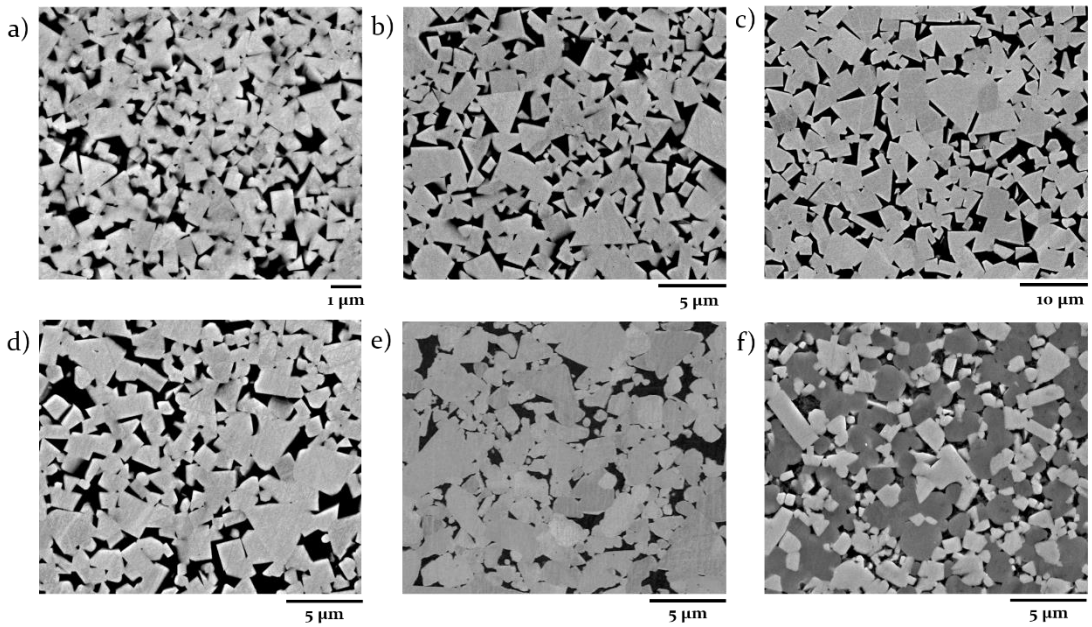

Figure 3.1. SEM images of the microstructures of the cemented carbide grades studied in this PhD thesis: a) WC-CoF; b) WC-CoM; c) WC-CoC; d) WC-CoNi; e) WC-NiMo; and f) WC-(W,Ti,Ta,Nb)C-Co.

3.2. Microscopy techniques

3.2.1. Scanning Electron Microscopy (SEM)

In material science, SEM is a widely used technique for characterization, given its high resolution and capacity to produce image of objects ranging from micro to nanometer scale [133]. In this work, SEM was used for microstructural characterization of the materials, and in combination with other powerful techniques such as FIB for sample preparation at the micrometer length scale and a nanoindenter, to perform in-situ the micromechanical testing in-situ.

A SEM consists of a source of electrons, a column where electrons travel, an electron detector, a sample chamber and a computerized display where images are viewed. In a SEM, an electron beam is produced by an electron gun and guided through a column by electromagnetic lenses towards the surface of the sample. The system is placed inside a chamber with ultra-high vacuum (around 10^{-6} torr), to avoid deacceleration of electrons. The system is provided with detectors that finally collect the electrons emitted by the sample because of the interaction with the electron beam. Thus, an image is formed with information of energy from detected electrons, their intensity and location of emission [133,134]. The electron beam interacts with atoms on the surface and inside the volume of the specimen. The two more important signals detected come from the secondary and backscattered electrons. The first provides contrast with variation of height in the surface of the samples; thus, the image in return correspond to the topography of the sample. The second reveals contrast between different elemental compositions according to their molecular weight. Thus, constitutive phases of a material can be identified because the variations in the grey tones found in the image [135].

3.2.2. Electron Back Scatter Diffraction (EBSD)

EBSD is a powerful technique used to identify individual grain orientation, constitutive phases of a sample and their distribution, and local texture, among others. In the present PhD thesis, EBSD was used to identify crystallographic orientation of the carbide phases that constituted the WC-(W,Ti,Ta,Nb)C-Co composite studied (see Article III). The technique is based in the generation and interpretation of diffraction patters from backscattered electrons in a SEM, also known as Kikuchi patterns. A scheme of the formation of Kikuchi patters is shown in Figure 3.2.

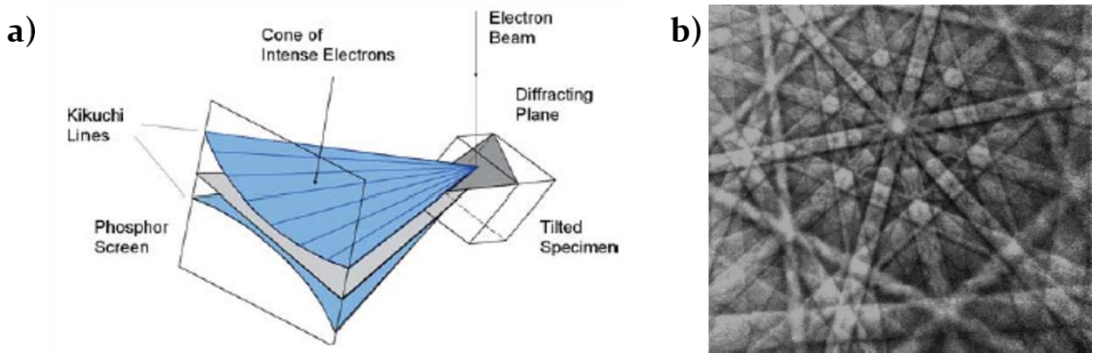

Figure 3.2. a) Scheme of the formation of Kikuchi patterns. b) Kikuchi pattern of Cadmium [136].

Backscatter diffraction from a crystalline material generates a pattern of parallel bright bands in a phosphor screen [136]. This pattern is characteristic of the crystallographic structure of the sample and the orientation of the sample region from where it was generated [137]. In the referred screen, the center of the projection is the point of incidence of the primary electron beam on the specimen surface, the

lattice planes can be thought as a pair of large angled cones stretched out to intersect the screen (as seen in Figure 3.2), and the plane between these cones is the projection of the diffracted plain in the screen [136].

3.2.3. Focused Ion Beam (FIB)

The FIB consists of a vacuum system and chamber, a liquid metal ion source, an ion column, a sample stage, detectors, gas delivery system and a computer to run the instrument (see Figure 3.3). It is usually incorporated to another analytical instrument as a SEM. Vacuum is necessary to avoid source contamination, prevent electrical discharges in the high voltage ion column as well as interaction of the ion beam with gas molecules [138]. Liquid Gallium (Ga) is commonly used as metal source, because it has a low melting point (29.8 °C) and low volatility at melting point. Therefore, there is no reaction or interfusion with tungsten needle, providing a long life of the metal source. Among other characteristics, Ga also has a low vapor pressure allowing its use in its pure form. Moreover, it has mechanical, electrical and vacuum properties which contribute to its selection as source of ions [138].

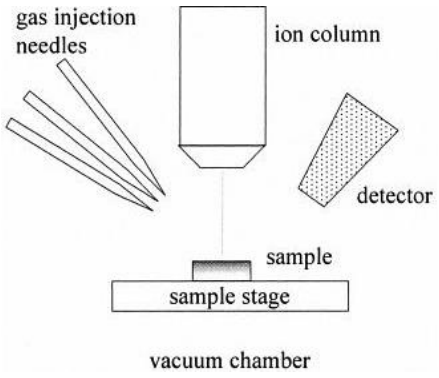

Figure 3.3. Scheme of the FIB system.

The Ga ions (Ga^+) are accelerated down the column with a voltage ranging between 5 and 50 keV. A set of condenser and objective lenses is used to determine the probe size and focus the beam towards the sample. A detector is employed to collect secondary electrons for image formation [138]. In the present PhD thesis, two SEM/FIB systems were used to mill micropillars and produce TEM lamellae from compressed micropillars. In the case of a dual beam system (SEM/FIB), the electron column is placed vertically in the chamber, whereas the ion column is located at an angle of 54° with respect to the first one. Thus, the area of interest is tilted, to co-focus both beams to the surface of the sample.

One important parameter to take into consideration when milling micropillars, is the aspect ratio - defined as the ratio between the pillar length (l_{pillar}), and its diameter at the top (d_{pillar}). Aspect ratio can magnify the pillar sink-in upon compression, leading to an inaccurate measurement of the pillar

deformation. Moreover, high aspect ratio can lead to premature buckling of the pillar. The second parameter to consider when milling micropillars is the taper angle. High taper angles can also lead to errors in estimation of stress from ideal strain-gradient free cylindrical micropillars. In this regard, it has been shown that an aspect ratio higher than 2 [55] and taper angle less than 5° [139] can have negligible effect in the calculated stress.

Considering the above restrictions, milling of micropillars for the present study was done by following a two-stage milling process. The first step was done with a dual beam Zeiss Neon 40 FIB/Field Emission SEM (FESEM) at Barcelona Research Center in Multiscale Science and Engineering (Universitat Politècnica de Catalunya). The second one was done with a FEI-Helios Nanolab 600 dual-beam FIB at the Italian Institute of Photonics and Nanotechnologies. In both cases a Ga^+ source operated at 30 kV was used. Micropillars were obtained by using a built-in pattern generator exploiting a "circle/donut" shape with user-defined parameters, including internal and external diameters, dwell time and number of passes. The incidence angle of the ions was 36° in both cases and the currents were 4 nA and 500 pA for the first and the second milling step, respectively. With this two-step methodology, interaction of Ga^+ was decreased, given the high exposure angle, low current and thus, less exposure time [140]. Dimensions of micropillars milled by FIB are summarized in Table 3.3.

Table 3.3. Summary of dimensions of micropillars milled by FIB in cemented carbides samples: micropillars diameter (d_{pillar}), aspect ratio (l_{pillar}/d_{pillar}) and taper angle (α).

Grade	d_{pillar} (μm)	l_{pillar}/d_{pillar}	α (°)
WC-Co (F)	2.1 ± 0.0	3.3 ± 0.1	3.4 ± 0.5
WC-Co (M)	1.1 ± 0.4	3.7 ± 1.4	2.5 ± 0.1
WC-Co (M)	2.0 ± 0.1	3.7 ± 0.1	3.1 ± 0.5
WC-Co (M)	3.8 ± 0.0	2.5 ± 0.0	1.8 ± 0.2
WC-Co (C)	1.9 ± 0.1	3.9 ± 0.2	3.1 ± 0.5
WC-CoNi	2.0 ± 0.0	3.6 ± 0.1	3.1 ± 0.3
WC-NiMo	2.0 ± 0.1	3.8 ± 0.3	3.4 ± 0.4
WC-(W,Ti,Ta,Nb)C-Co	1.6 ± 0.0	3.8 ± 0.2	1.4 ± 0.9

As mentioned above, a Zeiss Neon 40 FIB/FESEM was used to mill lamellae from the micropillars after uniaxial compression, to identify plastic deformation mechanisms in their constitutive phases by means of Transmission Electron Microscopy (TEM) inspection. Prior to milling the lamellae, a Pt layer was deposited in all the surface of the micropillars to avoid amorphization effect due to Ga^+ interaction with the samples. Once the lamellae were extracted from the sample and placed in a copper (Cu) grid, they were polished with a 5 kV current down to around 60 nm of thickness. The process followed to mill micropillars and lamellae with FIB is shown in Figure 3.4.

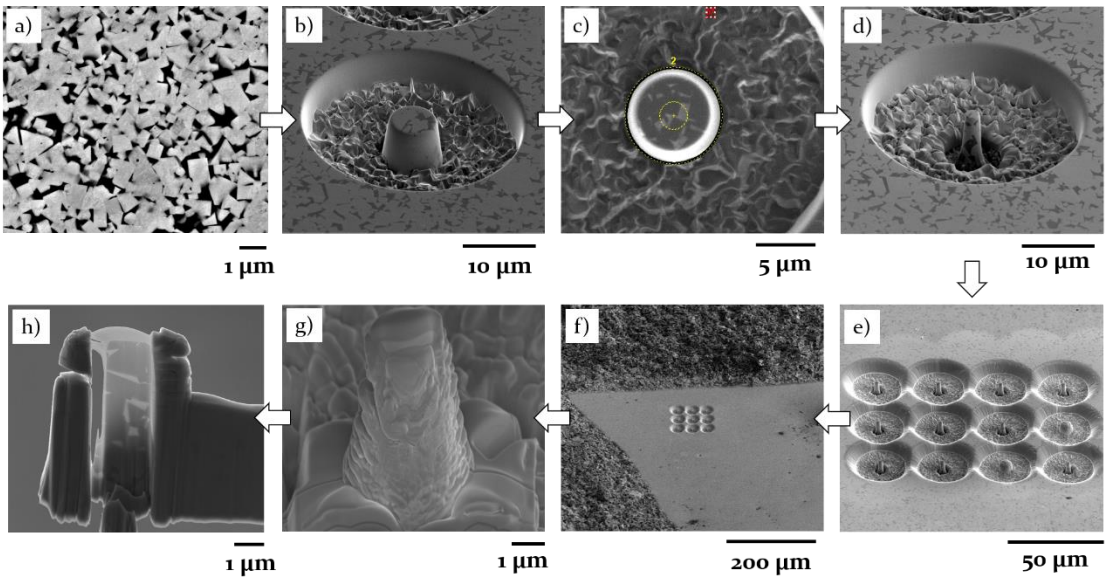

Figure 3.4. Image chart of the process followed to mill micropillars and TEM lamella with FIB system: a) selected surface of the material; b) micropillar produced with the first step of milling; c) selection of the dimensions of the second annular milling process; d) micropillar with final dimensions, obtained after second milling step; e) milling of 12 micropillars in each grade; f) image of the micropillars' matrix in the surface of the sample; g) micropillar selected for TEM lamella covered with Pt layer; and h) lamella produced from one micropillar milled in a WC-CoNi composite welded to a Cu grid.

3.2.4. Transmission Electron Microscopy (TEM)

TEM is an advance characterization technique commonly used in materials science to investigate microstructure and deformation mechanisms in the submicron and nanometer regime, given its high spatial and analytical resolution (down to 0.1 nm). In a TEM a high-energy beam of electrons interacts with a very thin samples (usually below 200 nm in thickness). A TEM uses both particle and wave characteristics of electrons to generate a tremendous range of signals so images, diffraction patterns (DPs) and several different types of spectra can be obtained [141].

In a conventional TEM, a thin specimen is irradiated with an electron beam of uniform current density (usually 100-200 kV), emitted in the electron gun by thermionic, Schottky or field emission. A condenser-lens system allows variation of the illumination aperture and the area of the specimen under consideration. The distribution of electrons intensity behind the sample is imaged with a lens system onto a fluorescent screen coupled with a fiber-optic plate to a charge coupled device (CCD) camera, to obtain a digital image [142]. A scheme of a TEM is shown in Figure 3.5.

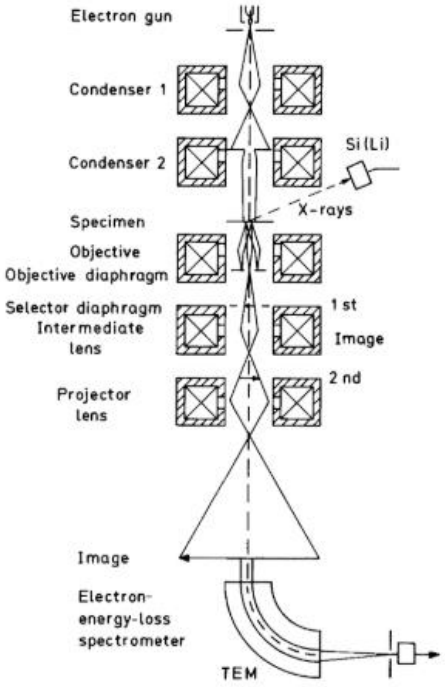

Figure 3.5. Schematic representation of the ray path in a TEM equipped for additional x-ray and electron energy-loss spectroscopy [142].

In TEM the primary beam generates a bright field image, whereas the Bragg-reflected beam generates a dark one. In crystalline materials, both beams give a diffraction contrast, which is important for imaging of crystal defects [142]. Furthermore, DPs resulting from variations of the diffracted beams in different regions of the specimen, allows to relate crystallography features to attained images [141]. In this PhD thesis a JEOL JEM-2100 LaB6 TEM unit at Scientific and Technological Center of Universitat de Barcelona was used. The equipment was operated at 200 kV. Bright and dark field TEM images were used to discern deformation features in constitutive phases of medium-grained WC-Co, WC-CoNi and WC-NiMo cemented carbide grades.

3.3. Uniaxial compression of micropillars

Uniaxial compression tests were done in-situ, using a nanoindenter INSEM Nanomechanics placed inside a high-resolution field-emission-gun scanning electron microscope (FEG-SEM, LEO 35, Zeiss), and equipped with a flat-diamond punch of 5 μm in nominal diameter. The equipment was facilitated by the Italian National Agency for New Technologies, Energy and Sustainable Economic Development (ENEA). The experimental setup can be seen in Figure 3.6.

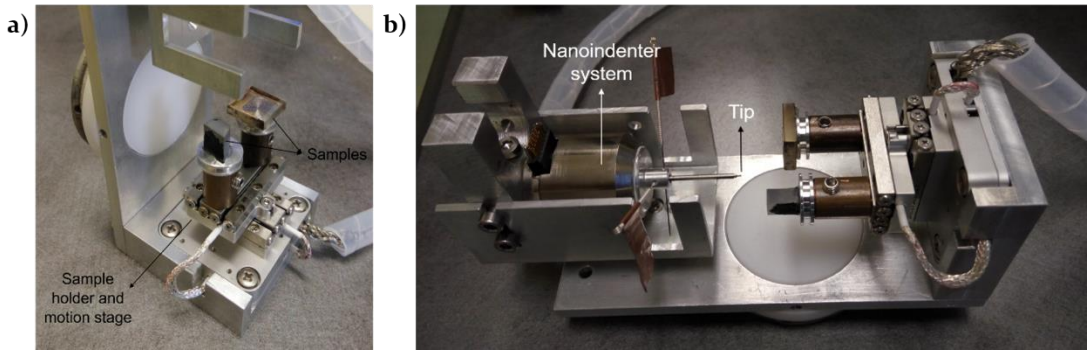

Figure 3.6. Nanoindentation system mounted in a SEM holder: a) detail of motion station and location of samples; and b) detail of nanoindentation system and nanoindentation tip.

Uniaxial compression tests were carried under displacement-control mode. Maximum nanoindentation depth into the sample was set to have elastic and plastic response, avoiding catastrophic failure. Load-displacement (*P-h*) data was continuously recorded during the tests. Nominal stresses and strains were directly calculated from the load-displacement data. Effective elastic deformation of both the indenter and the bulk material below the micropillar was extracted, to calculate strains of micropillars. In doing so, an approach derived by Sneddon [143,144] was used, according to the following expression:

$$x_{Sneddon} = (1-\nu_i^2/E_i)*(F_{meas}/d_t) + (1-\nu_b^2/E_b)*(F_{meas}/d_b) \quad \text{Equation 8}$$

where $x_{Sneddon}$ is the displacement corrected by the Sneddon's approach, which is subtracted from the total displacement; F_{meas} is the measured force; d_t and d_b are the diameters of the micropillar at the top and bottom respectively; and Young's modulus and Poisson's ratio of the diamond tip, E_i and ν_i, are 1141 GPa and 0.07 respectively [145]; Young's modulus of the bulk is E_b, taken to be 577 GPa for WC-Co grades and WC-NiMo one, 593 GPa for WC-CoNi, and 475 GPa for WC-(W,Ti,Ta,Nb)-Co. Poisson's ratio ν_b was considered as 0.24 for all grades [146]. Calibration of the equipment was done on fused silica micropillars of known elastic modulus (72 GPa) [145].

Nominal stresses (σ) and strains (ε) values were directly determined from the *P-h* curve at 1 μm depth from the micro-pillars surface. This was done to avoid milling effects (e.g. round shape of the pillar) and/or because such location is the place where the maximum deformation is located during the compression process - in agreement with protocol followed by the scientific community addressing micropillar compression testing (e.g. [57,119,147]) - according to the following expressions:

$$\sigma = P/A_0 \quad \text{Equation 9}$$

$$\varepsilon = (L_0-h)/L_0 \quad \text{Equation 10}$$

where P and h are the load and displacement respectively from the P-h curve, A_o is the area of the micropillars at 1 μm depth, and L_o is the initial length of the micropillars. Stress-strain curves were drawn with the software OriginLab - OriginPro version 9.1.

The characteristic microstructural length selected to evaluate size effect in uniaxial compression of micropillars tests was WC mean grain size. Sizes of micropillars were selected according to the ratio between diameter of micropillar and WC mean grain size (d_{pillar}/d_{WC}). On one hand, a WC-Co grade with medium WC grain size (WC-CoM) was selected to mill micropillars of 1, 2 and 4 μm in diameter, to evaluate the effect of the sample size on its micromechanical response. On the other hand, micropillars of 2 μm in diameter were milled in fine, medium and coarse WC-Co grades, to evaluate the effect of the volume fraction of each constitutive phase within the micropillar, on the micromechanical response. Finally, based on the results obtained from the size effect study, a d_{pillar}/d_{WC} ratio of 2 was selected to evaluate the effect of partial and total substitution of Co as binder, and partial substitution of WC. A summary of $d_{pillar}/d_{carbide}$ ratios selected for each stage of the study may be found in Table 3.4.

Table 3.4. Ratio diameter of micropillar and WC mean grain size ($d_{pillar}/d_{carbide}$) selected in this study to evaluate sample size effect on the micromechanical response of cemented carbides by means of uniaxial compression of micropillars.

d_{pillar}	$d_{pillar}/d_{carbide}$					
	WC-CoF	**WC-CoM**	**WC-CoC**	**WC-CoNiM**	**WC-NiMoM**	**WC-(W,Ti,Ta,Nb)C-CoM**
4		3.6				
2	5.1	1.8	0.9	1.9	2.0	2.0
1		0.9				

3.4. Massive nanoindentation

A massive nanoindentation protocol was followed to evaluate the feasibility to determine the intrinsic hardness of the constitutive phases and the plastic flow of the binder within the complex alloy WC-(W,Ti,Ta,Nb)C-Co. Maximum indentation depth of 200 nm was considered suitable to avoid any size or scale effect, based on the study done by Roa *et al.* [148]. In such study it was shown that indentation imprint and plastic field were confined within WC particles, in a WC-Co grade with WC mean grain size of 1.1 ± 0.7 μm.

Nanoindentation measurements were done with a Nanoindenter XP (MTS) using the continuous stiffness measurement module (CSM) with a Berkovich tip. Before performing the nanoindentations, the contact area of the tip was calibrated with fused silica with known value of modulus, E=72 GPa and a

Poisson's ratio of around 0.17. Intrinsic hardness of each constitutive phase was determined from the *P-h* curves, following the Oliver and Pharr method [145].

Hardness and elastic modulus of the composite bulk material was determined before massive nanoindentation testing. Arrays of 3 x 3 nanoindentations were done with a penetration depth of 2000 nm (or until reaching a maximum applied load of 650 mN) and 50 μm of distance between each indentation to guarantee that no overlapping of the residual imprints occurred.

To determine the intrinsic hardness of the constitutive phases of the cemented carbide grade, two arrays of 20 x 20 nanoindentations were done with a maximum displacement into surface of 200 nm and a distance between nanoindentations of 3 μm, assuring that the number of measurements obtained were sufficient to obtain representative data to be analyzed by means of the statistical method followed.

3.4.1. Statistical method for determination of intrinsic hardness of constitutive phases

Hardness for each constitutive phases was determine following the statistical method proposed by Ulm *et al.* [131,149,150]. A large data from indentations arrays was analyzed and subsequently deconvoluted by approximating the distribution of the mechanical properties (p_i) to a Gaussian distribution, described by the following expression:

$$p_i = \frac{1}{\sqrt{2\pi{\sigma_i}^2}} exp^{\left(-\frac{(x-\mu_i)^2}{2{\sigma_i}^2}\right)} \quad \text{Equation 11}$$

where σ_i is standard deviation and μ_i is the arithmetic mean value of hardness (H) for all indentation N_i in the phase i.

Mean values of μ_i and σ_i were acquired from fitting the cumulative distribution function (CDF) using a sigmoid shape error function, written as Equation 12 [91,151].

$$CDF = \sum_i \frac{1}{2} f_i erf\left(\frac{x-x_i}{\sqrt{2\sigma i}}\right) \quad \text{Equation 12}$$

where

$$\sum_{i=1}^{n} f_i = 1 \quad \text{Equation 13}$$

The fitting process was programmed to be completed when the chi-square χ^2 tolerance is less than 1.10^{-15}.

Software Origin® Pro 9.1 was used to analyze the data obtained. Fitting and deconvolution process was done by following Equation 14, considering the following constitutive phases: WC basal, WC prismatic, mixed cubic carbide (W,Ti,Ta,Nb)C and Co binder.

$$CDF = \frac{1}{2}f_1\left(1 + erf\left(\frac{x-x_1}{\sqrt{2\sigma_1}}\right)\right) + \frac{1}{2}f_2\left(1 + erf\left(\frac{x-x_2}{\sqrt{2\sigma_2}}\right)\right) + \frac{1}{2}f_3\left(1 + erf\left(\frac{x-x_3}{\sqrt{2\sigma_3}}\right)\right) + \frac{1}{2}(1 - f_1 - f_2 - f_3)\left(1 + erf\left(\frac{x-x_4}{\sqrt{2\sigma_4}}\right)\right)$$ Equation 14

3.4.2. Flow stress (σ_{flow}) of the binder phase

Experimental hardness values for the constrained binder obtained by statistical analysis of data resulting from nanoindentation tests show wide scatter due to the uneven local constrain imposed by carbide particles. Thus, they cannot be used directly as reliable data for modelling and/or microstructural design optimization. However, it is a basic parameter to be used in determination of the flow stress (σ_{flow}) for the constrained metallic binder which have been proved to give reliable results [113].

σ_{flow} for the constrained binder was determined from the hardness value obtained by modification of the statistical method. In doing so, it was assumed to be the ratio between the measured Vickers hardness (HV) and a constraint factor (ψ) reported to be in the range of 3-4 for WC-Co hardmetals (depending on binder content or carbide grain size) [152]. The influence of the carbide particles underlying binder pools in which an indentation imprint was found, was evaluated by means of thin film models [153]. Finally, results were compared to plastic deformation phenomena (pop-ins) observed in σ-ε curves previously obtained by means of uniaxial compression of micropillars.

References

[1] H.E. Exner, Physical and chemical nature of cemented carbides, Int. Mater. Rev. 4 (1979) 1149–73. doi:10.1179/imtr.1979.24.1.149.

[2] G.. Upadhyaya, Nature and properties of refractory carbides, Nova Science Publishers, Inc., Commack, NY, 1996.

[3] Hyperion Materials & Technologies, All about cemented carbide, (2019). http://www.allaboutcementedcarbide.com/ (accessed August 22, 2019).

[4] H.M. Ortner, P. Ettmayer, H. Kolaska, The history of the technological progress of hardmetals, Int. J. Refract. Met. Hard Mater. 44 (2014) 148–159. doi:10.1016/j.ijrmhm.2013.07.014.

[5] P. Ettmayer, H. Kolaska, H.M. Ortner, History of hardmetals, in: V. Sarin, D. Mari, L. Llanes, C.E. Nebel (Eds.), Compr. Hard Mater. Vol. 1-3, Elsevier Ltd., Oxford, UK, 2014: pp. 3–27. doi:10.1017/CBO9781107415324.004.

[6] G.S. Upadhyaya, Cemented tungsten carbides: production, properties and testing, Noyes Publications, New Jersey, USA, 1998.

[7] K. Brookes, There's more to hard materials than tungsten carbide alone, Met. Powder Rep. 66 (2011) 36–45. doi:10.1016/S0026-0657(11)70062-5.

[8] ITIA, International tungsten industry association, (2011). https://www.itia.info/ (accessed May 25, 2019).

[9] B. North, Global trends in hard materials, in: L. Sigl, P. Rödhammer, S. Wildner (Eds.), Proc. 17th Int. Plansee Semin. Plansee Met. AG, Austria, 2005.

[10] S. Norgren, J. García, A. Blomqvist, L. Yin, Trends in the P/M hard metal industry, Int. J. Refract. Met. Hard Mater. 48 (2015) 31–45. doi:10.1016/j.ijrmhm.2014.07.007.

[11] K. Brookes, Plansee Seminar 2017. Opening Session - Global hardmetal trends, Met. Powder Rep. 72 (2017) 301–308. doi:http://dx.doi.org/10.1016/j.mprp.2017.08.001.

[12] G. Upadhyaya, Materials science of cemented carbides — an overview, Mater. Des. 22 (2001) 483–489. doi:10.1016/S0261-3069(01)00007-3.

[13] L. Prakash, Developments in tungsten carbide-cobalt cemented carbides, Int. Powder Metall. Dir. (2008) 131–148.

[14] S. Lay, J.M. Missiaen, Microstructure and morphology of hardmetals, in: V.K. Sarin, D. Mari, L. Llanes, C.E. Nebel (Eds.), Compr. Hard Mater., Elsevier Ltd., Oxford, UK, 2014: pp. 91–117.

[15] J.R. Davis, ed., ASM Specialty Handbook: Tool Materials, ASM International, 1995.

[16] A. Petersson, Cemented carbide sintering: constitutive relations and microstructural evolution (Ph.D. thesis), Royal Institute of Technology (KTH), Stocholm, Sweden, 2004.

[17] L. Prakash, Fundamentals and general applications of hardmetals, in: V.K. Sarin, D. Mari, L. Llanes, C.E. Nebel (Eds.), Compr. Hard Mater. Vol. 1, Elsevier Ltd, UK, 2014: pp. 29–90.

[18] K. Mannesson, WC grain growth during sintering of cemented carbides, KTH Royal Institute of Technology, 2011. doi:10.1016/j.ijrmhm.2005.11.009.

[19] J. Gurland, New scientific approaches to development of tool materials, Int. Mater. Rev. 33 (1988) 151–166. doi:10.1179/imr.1988.33.1.151.

[20] B. Roebuck, E.A. Almond, A.M. Cottenden, The influence of composition, phase-transformation and varying the relative fcc and hcp phase content on the properties of dilute Co-W-C alloys, Mater. Sci. Eng. 66 (1984) 179–194. doi:10.1016/0025-5416(84)90179-4.

[21] Ad hoc Working Group on defining critical raw materials, Report on critical raw materials for the EU, 2014. http://mima.geus.dk/report-on-critical-raw-materials_en.pdf (accessed June 4, 2019).

[22] M. Grilli, T. Bellezze, E. Gamsjäger, A. Rinaldi, P. Novak, S. Balos, R. Piticescu, M. Ruello, M.L. Grilli, T. Bellezze, E. Gamsjäger, A. Rinaldi, P. Novak, S. Balos, R.R. Piticescu, M.L. Ruello, Solutions for Critical Raw Materials under Extreme Conditions: A Review, Materials (Basel). 10 (2017) 285. doi:https://doi.org/10.3390/ma10030285.

[23] European Comission, Strategic implementation plan for the European Innovation Partnership on raw materials Part I, 2019. https://ec.europa.eu/growth/tools-databases/eip-raw-materials/en/system/files/ged/20130731_SIP Part I complet clean.pdf (accessed June 4, 2019).

[24] Critical raw materials substitution profiles, 2013. http://cdn.awsripple.com/www.criticalrawmaterials.eu/ (accessed June 4, 2019).

[25] C.M. Fernandes, A.M.R. Senos, Cemented carbide phase diagrams: A review, Int. J. Refract. Met. Hard Mater. 29 (2011) 405–418. doi:10.1016/j.ijrmhm.2011.02.004.

[26] REACH, Registration, Evaluation, Authorisation and Restriction of Chemicals (REACH) - CLH report for cobalt, 2019.

[27] National toxicology program (NTP), 14th Report on carcinogens, 2016.

[28] M. Woydt, H. Mohrbacher, J. Vleugels, S. Huang, Potentials of niobium carbide (NBC) as cutting tools and for wear protection, Ceram. Eng. Sci. Proc. 38 (2018) 99–111. doi:10.1002/9781119474678.ch10.

[29] C.H. Vasel, A.D. Krawitz, E.F. Drake, E.A. Kenik, Binder deformation in WC-(Co, Ni) cemented carbide composites, Metall. Trans. A. 16 (1985) 2309–2317. doi:10.1007/BF02670431.

[30] V.K. Sarin, T. Johannesson, On the deformation of WC–Co cemented carbides, Met. Sci. 9 (2010) 472–476. doi:10.1179/030634575790444531.

[31] C.T. Peters, S.M. Brabyn, Properties of nickel-substitued hardmetals and their performance in hard rock drill bits, Met. Powder Rep. 42 (1987) 863–865.

[32] A.M. Human, I.T. Northrop, S.B. Luyckx, M.N. James, A comparison between cemented carbides containing Cobalt- and Nickel-based binders, J. Hard Mater. 2 (1991) 245–256.

[33] J.M. Tarragó, J.J. Roa, V. Valle, J. Marshall, L. Llanes, Fracture and fatigue behavior of WC-Co and WC-CoNi cemented carbides, Int. J. Refract. Met. Hard Mater. 49 (2015) 184–191. doi:10.1016/j.ijrmhm.2014.07.027.

[34] J.M. Tarragó, C. Ferrari, B. Reig, D. Coureaux, L. Schneider, L. Llanes, Mechanics and mechanisms of fatigue in a WC-Ni hardmetal and a comparative study with respect to WC-Co hardmetals, Int. J. Fatigue. 70 (2015) 252–257. doi:10.1016/j.ijfatigue.2014.09.011.

[35] S. Ekemar, L. Lindholm, T. Hartzell, Aspects of nickel as a binder metal in WC-based cemented carbides, in: Proc. 10th Plansee-Seminar, 1981: pp. 1–477.

[36] E. Kny, L. Schmid, New hardmetal alloys with improved erosion and corrosion resistance, Int. J. Refract. Met. Hard Mater. 6 (1987) 145–148.

[37] V.A. Tracey, Nickel in hardmetals, Refract. Met. Hard Mater. 11 (1992) 137–149.

[38] B. Roebuck, E.A. Almond, Deformation and fracture processes and the physical metallurgy of WC-Co hardmetals, Int. Mater. Rev. 33 (1988) 90–112. doi:10.1179/095066088790324094.

[39] J. García, V. Collado Ciprés, A. Blomqvist, B. Kaplan, Cemented carbide microstructures: a review, Int. J. Refract. Met. Hard Mater. 80 (2019) 40–68. doi:10.1016/j.ijrmhm.2018.12.004.

[40] G.E. Spriggs, A history of fine grained hardmetal, Int. J. Refract. Met. Hard Mater. 13 (1995) 241–255. doi:10.1016/0263-4368(95)92671-6.

[41] L.H. Zeferino, A.C. Buriti, S.N. Monteiro, A.G.P. da Silva, Determination of the WC grain size in hardmetals using stereology – A critical analysis, Int. J. Refract. Met. Hard Mater. 26 (2008) 367–371. doi:10.1016/j.ijrmhm.2007.08.011.

[42] Metallographic determination of microstructure. Part 2: measurement of WC grain size, in: ISO 4499-2 2008, Hardmetals, Geneva, 2008.

[43] M. Savard, The characterization of cemented carbides by automated image analysis, Jom. 60 (2008) 23–28. doi:https://doi.org/10.1007/s11837-008-0043-x.

[44] M. Brieseck, W. Lengauer, B. Gneiß, K. Wagner, S. Wagner, A straightforward method for analysing the grain-size distribution in tungsten carbide - cobalt hardmetals, Microchim. Acta. 168 (2010) 309–316. doi:10.1007/s00604-010-0294-4.

[45] J.M. Tarragó, D. Coureaux, Y. Torres, F. Wu, I. Al-Dawery, L. Llanes, Implementation of an effective time-saving two-stage methodology for microstructural characterization of cemented carbides, Int. J. Refract. Met. Hard Mater. 55 (2016) 80–86. doi:10.1016/j.ijrmhm.2015.10.006.

[46] H.C. Lee, J. Gurland, Hardness and deformation of cemented tungsten carbide, Mater. Sci. Eng. 33 (1978) 125–133. doi:10.1016/0025-5416(78)90163-5.

[47] S. Luyckx, A. Love, The dependence of the contiguity of WC on Co content and its independence from WC grain size in WC-Co alloys, Int. J. Refract. Met. Hard Mater. 24 (2006) 75–79. doi:10.1016/j.ijrmhm.2005.04.012.

[48] A. V. Shatov, S.S. Ponomarev, S.A. Firstov, R. Warren, The contiguity of carbide crystals of different shapes in cemented carbides, Int. J. Refract. Met. Hard Mater. 24 (2006) 61–74. doi:10.1016/j.ijrmhm.2005.03.003.

[49] D. Coureaux, Comportamiento mecánico de carburos cementados WC-Co: Influencia de la microestructura en la resistencia a la fractura, la sensibilidad a la fatiga y la tolerancia al daño inducido bajo solicitaciones de contacto, PhD Thesis Universitat Politècnica de Catalunya, 2012.

[50] J.B. Pethicai, R. Hutchings, W.C. Oliver, Hardness measurement at penetration depths as small as 20 nm, Philos. Mag. A. 48 (1983) 593–606. doi:10.1080/01418618308234914.

[51] G. Binnig, H. Rohrer, C. Gerber, E. Weibel, Surface studies by scanning tunneling microscopy, Phys. Rev. Lett. 49 (1982) 57–61. doi:10.1103/physrevlett.49.57.

[52] B. Bhushan, Springer handbook of nanotechnology, Springer Science & Business Media, 2010.

[53] M.D. Uchic, D.M. Dimiduk, J.N. Florando, W.D. Nix, Sample dimensions influence strength and crystal plasticity, Science. 305 (2004) 986–989. doi:10.1126/science.1098993.

[54] J.R. Greer, J.T.M. De Hosson, Plasticity in small-sized metallic systems: Intrinsic versus extrinsic size effect, Prog. Mater. Sci. 56 (2011) 654–724. doi:10.1016/j.pmatsci.2011.01.005.

[55] H. Zhang, B.E. Schuster, Q. Wei, K.T. Ramesh, The design of accurate micro-compression experiments, Scr. Mater. 54 (2006) 181–186. doi:10.1016/j.scriptamat.2005.06.043.

[56] J.L. Stewart, L. Jiang, J.J. Williams, N. Chawla, Prediction of bulk tensile behavior of dual phase stainless steels using constituent behavior from micropillar compression experiments, Mater. Sci. Eng. A. 534 (2012) 220–227. doi:10.1016/j.msea.2011.11.062.

[57] D.M. Dimiduk, M.D. Uchic, T.A. Parthasarathy, Size-affected single-slip behavior of pure nickel microcrystals, Acta Mater. 53 (2005) 4065–4077. doi:10.1016/j.actamat.2005.05.023.

[58] G. Dehm, B.N. Jaya, R. Raghavan, C. Kirchlechner, Overview on micro- and nanomechanical testing: New insights in interface plasticity and fracture at small length scales, Acta Mater. 142 (2018) 248–282. doi:10.1016/j.actamat.2017.06.019.

[59] B. Girault, A.S. Schneider, C.P. Frick, E. Arzt, Strength effects in micropillars of a dispersion strengthened superalloy, Adv. Eng. Mater. 12 (2010) 385–388. doi:10.1002/adem.201000089.

[60] P. Hosemann, C. Shin, D. Kiener, Small scale mechanical testing of irradiated materials, J. Mater. Res. 30 (2015) 1231–1245. doi:10.1557/jmr.2015.26.

[61] B. AlMangour, J.-M. Yang, Understanding the deformation behavior of 17-4 precipitate hardenable stainless steel produced by direct metal laser sintering using micropillar compression and TEM, Int. J. Adv. Manuf. Technol. 90 (2016) 119–126. doi:10.1007/s00170-016-9367-9.

[62] W. Chen, J. Zhang, S. Cao, Y. Pan, M. Huang, Q. Hu, Q. Sun, L. Xiao, J. Sun, Strong deformation anisotropies of ω -precipitates and strengthening mechanisms in Ti-10V-2Fe-3Al alloy micropillars: Precipitates shearing vs precipitates disordering, Acta Mater. 117 (2016) 68–80. doi:10.1016/j.actamat.2016.06.065.

[63] K.S. Ng, A.H.W. Ngan, Deformation of micron-sized aluminium bi-crystal pillars, Philos. Mag. 89 (2009) 3013–3026. doi:10.1080/14786430903164614.

[64] A. Kunz, S. Pathak, J.R. Greer, Size effects in Al nanopillars: Single crystalline vs. bicrystalline, Acta Mater. 59 (2011) 4416–4424. doi:10.1016/j.actamat.2011.03.065.

[65] N. Kheradmand, H. Vehoff, Orientation gradients at boundaries in micron-sized bicrystals, Adv. Eng. Mater. 14 (2012) 153–161. doi:10.1002/adem.201100242.

[66] P.J. Imrich, C. Kirchlechner, C. Motz, G. Dehm, Differences in deformation behavior of bicrystalline Cu micropillars containing a twin boundary or a large-angle grain boundary, Acta Mater. 73 (2014) 240–250. doi:10.1016/j.actamat.2014.04.022.

[67] N.V. Malyar, J.-S. Micha, G. Dehm, C. Kirchlechner, Dislocation-twin boundary interaction in small scale Cu bi-crystals loaded in different crystallographic directions, Acta Mater. 129 (2017) 91–97. doi:10.1016/j.actamat.2017.02.067.

[68] N.V. Malyar, J.S. Micha, G. Dehm, C. Kirchlechner, Size effect in bi-crystalline micropillars with a penetrable high angle grain boundary, Acta Mater. 129 (2017) 312–320. doi:10.1016/j.actamat.2017.03.003.

[69] D. Bhattacharyya, N.A. Mara, P. Dickerson, R.G. Hoagland, A. Misra, Compressive flow behavior of Al–TiN multilayers at nanometer scale layer thickness, Acta Mater. 59 (2011) 3804–3816. doi:10.1016/j.actamat.2011.02.036.

[70] D. Kupka, E.T. Lilleodden, Mechanical testing of solid–solid interfaces at the microscale, Exp. Mech. 52 (2012) 649–658. doi:10.1007/s11340-011-9530-z.

[71] S. Lotfian, M. Rodríguez, K.E. Yazzie, N. Chawla, J. Llorca, J.M. Molina-Aldareguía, High temperature micropillar compression of Al/SiC nanolaminates, Acta Mater. 61 (2013) 4439–4451. doi:10.1016/j.actamat.2013.04.013.

[72] R. Raghavan, J.M. Wheeler, D. Esqué-de los Ojos, K. Thomas, E. Almandoz, G.G. Fuentes, J. Michler, Mechanical behavior of Cu/TiN multilayers at ambient and elevated temperatures: Stress-assisted diffusion of Cu, Mater. Sci. Eng. A. 620 (2015) 375–382. doi:10.1016/j.msea.2014.10.023.

[73] J.M. Wheeler, R. Raghavan, V. Chawla, J. Zechner, I. Utke, J. Michler, Failure mechanisms in metal–metal nanolaminates at elevated temperatures: Microcompression of Cu–W multilayers, Scr. Mater. 98 (2015) 28–31. doi:10.1016/j.scriptamat.2014.11.007.

[74] J. Wehrs, M.J. Deckarm, J.M. Wheeler, X. Maeder, R. Birringer, S. Mischler, J. Michler, Elevated temperature, micro-compression transient plasticity tests on nanocrystalline Palladium-Gold: Probing activation parameters at the lower limit of crystallinity, Acta Mater. 129 (2017) 124–137. doi:10.1016/j.actamat.2017.02.045.

[75] D. Di Maio, S.G. Roberts, Measuring fracture toughness of coatings using focused-ion-beam-machined microbeams, J. Mater. Res. 20 (2005) 299–302. doi:doi:10.1557/JMR.2005.0048.

[76] K. Matoy, H. Schönherr, T. Detzel, T. Schöberl, R. Pippan, C. Motz, G. Dehm, A comparative micro-cantilever study of the mechanical behavior of silicon based passivation films, Thin Solid Films. 518 (2009) 247–256. doi:10.1016/j.tdf.2009.07.143.

[77] F. Iqbal, J. Ast, M. Göken, K. Durst, In situ micro-cantilever tests to study fracture properties of NiAl single crystals, Acta Mater. 60 (2012) 1193–1200. doi:10.1016/j.actamat.2011.10.060.

[78] S. Wurster, C. Motz, R. Pippan, Characterization of the fracture toughness of micro-sized tungsten single crystal notched specimens, Philos. Mag. 92 (2012) 1803–1825. doi:10.1080/14786435.2012.658449.

[79] S. Liu, J.M. Wheeler, P.R. Howie, X.T. Zeng, J. Michler, W.J. Clegg, Measuring the fracture resistance of hard coatings, Appl. Phys. Lett. 102 (2013) 171907. doi:10.1063/1.4803928.

[80] B.N. Jaya, C. Kirchlechner, G. Dehm, Can microscale fracture tests provide reliable fracture toughness values? A case study in silicon, J. Mater. Res. 30 (2015) 686–698. doi:10.1557/jmr.2015.2.

[81] S. Korte-Kerzel, Microcompression of brittle and anisotropic crystals: recent advances and current challenges in studying plasticity in hard materials, MRS Commun. 7 (2017) 109–120. doi:10.1557/mrc.2017.15.

[82] K. Jia, T.E. Fischer, B. Gallois, Microstructure, hardness and toughness of nanostructured and conventional WC-Co composites, Nanostructured Mater. 10 (1998) 875–891. doi:10.1016/S0965-9773(98)00123-8.

[83] W.D. Schubert, H. Neumeister, G. Kinger, B. Lux, Hardness to toughness relationship of fine-grained WC-Co hardmetals, Int. J. Refract. Met. Hard Mater. 16 (1998) 133–142. doi:10.1016/S0263-4368(98)00028-6.

[84] B. Roebuck, Extrapolating hardness-structure property maps in WC/Co hardmetals, Int. J. Refract. Met. Hard Mater. 24 (2006) 101–108. doi:10.1016/j.ijrmhm.2005.04.021.

[85] R.W. Armstrong, The hardness and strength properties of WC-Co composites, Materials (Basel). 4 (2011) 1287–1308. doi:10.3390/ma4071287.

[86] T. Takahashi, E.J. Freise, Determination of the slip systems in single crystals of tungsten monocarbide, Philos. Mag. 12 (1965) 1–8. doi:10.1080/14786436508224941.

[87] D.N. French, D.A. Thomas, Hardness anisotropy and slip in WC crystals. Trans. AIME, vol. 233, May 1965, pp. 950-952, Trans. Metall. Soc. Aime. 233 (1965) 950–952.

[88] L. Pons, Plastic properties in tungsten monocarbide, in: F. Vahldiek, W. Mersol, A. Stanley (Eds.), Anisotropy Single-Crystal Refract. Compd. Vol. 2, Plenum Press, New York, 1968: pp. 393–444. doi:10.1007/978-1-4899-5307-0.

[89] M. Lee, High temperature hardness of tungsten carbide, Metall. Mater. Trans. A. 14 (1983) 1625–1629. doi:10.1007/bf02654390.

[90] N. Cuadrado, D. Casellas, L. Llanes, I. Gonzalez, J. Caro, Effect of crystal anisotropy on the mechanical properties of WC embedded in WC-Co cemented carbides, Proc. Euro Int. Powder Metall. Congr. Exhib. Euro PM 2011. 1 (2011) 215–220.

[91] E. Rayón, V. Bonache, M.D. Salvador, J.J. Roa, E. Sánchez, Hardness and Young's modulus distributions in atmospheric plasma sprayed WC–Co coatings using nanoindentation, Surf. Coatings Technol. 205 (2011) 4192–4197. doi:10.1016/j.surfcoat.2011.03.012.

[92] B. Roebuck, P. Klose, K.P. Mingard, Hardness of hexagonal tungsten carbide crystals as a function of orientation, Acta Mater. 60 (2012) 6131–6143. doi:10.1016/j.actamat.2012.07.056.

[93] A. Duszová, R. Halgaš, M. Bľanda, P. Hvizdoš, F. Lofaj, J. Dusza, J. Morgiel, Nanoindentation of WC-Co hardmetals, J. Eur. Ceram. Soc. 33 (2013) 2227–2232. doi:10.1016/j.jeurceramsoc.2012.12.018.

[94] O. Rüdiger, D. Hirschfeld, A. Hoffmann, J. Kolaska, G. Ostermann, J. Willbrand, Composition and properties of the binder metal in cobalt bonded tungsten carbide, in: Mod. Dev. Powder Metall., Springer US, Boston, MA, 1971: pp. 215–224. doi:10.1007/978-1-4615-8963-1_16.

[95] J.J. Roa, E. Jiménez-Piqué, J.M. Tarragó, D.A. Sandoval, A. Mateo, J. Fair, L. Llanes, Hall-Petch strengthening of the constrained metallic binder in WC–Co cemented carbides: Experimental assessment by means of massive nanoindentation and statistical analysis, Mater. Sci. Eng. A. (2016). doi:10.1016/j.msea.2016.09.020.

[96] A.G. Evans, R.M. McMeeking, On the toughening of ceramics by strong reinforcements, Acta Metall. 34 (1986) 2435–2441. doi:10.1016/0001-6160(86)90146-X.

[97] M.F. Ashby, F.J. Blunt, M. Bannister, Flow characteristics of highly constrained metal wires, Acta Metall. 37 (1989) 1847–1857. doi:10.1016/0001-6160(89)90069-2.

[98] J. Riesch, J.Y. Buffiere, T. Höschen, M. Di Michiel, M. Scheel, C. Linsmeier, J.H. You, In situ synchrotron tomography estimation of toughening effect by semi-ductile fibre reinforcement in a tungsten-fibre-reinforced tungsten composite system, Acta Mater. 61 (2013) 7060–7071. doi:10.1016/j.actamat.2013.07.035.

[99] J.M. Tarragó, E. Jimenez-Piqué, M. Turón-Viñas, L. Rivero, I. Al-Dawery, L. Schneider, L. Llanes, Fracture and fatigue behavior of cemented carbides: 3D focused ion beam tomography of crack-microstructure interactions, Int. J. Powder Metall. 50 (2014) 33–42. http://hdl.handle.net/2117/26072.

[100] V. Livescu, B. Clausen, J.W. Paggett, A.D. Krawitz, E.F. Drake, M.A.M. Bourke, Measurement and modeling of room temperature co-deformation in WC-10wt.% Co, Mater. Sci. Eng. A. 399 (2005) 134–140. doi:10.1016/j.msea.2005.02.024.

[101] J.W. Paggett, A.D. Krawitz, E.F. Drake, M.A.M. Bourke, V. Livescu, B. Claussen, D.W. Brown, In situ loading response of WC-Ni: Origins of toughness, Int. J. Refract. Met. Hard Mater. 24 (2006) 122–128. doi:10.1016/j.ijrmhm.2005.06.005.

[102] A.D. Krawitz, A.M. Venter, E.F. Drake, S.B. Luyckx, B. Clausen, Phase response of WC-Ni to cyclic compressive loading and its relation to toughness, Int. J. Refract. Met. Hard Mater. 27 (2009) 313–316. doi:10.1016/j.ijrmhm.2008.11.010.

[103] A.D. Krawitz, E.F. Drake, B. Clausen, The role of residual stress in the tension and compression response of WC–Ni, Mater. Sci. Eng. A. 527 (2010) 3595–3601. doi:10.1016/j.msea.2010.02.046.

[104] A. Krawitz, E. Drake, Residual stresses in cemented carbides - An overview, Int. J. Refract. Met. Hard Mater. 49 (2015) 27–35. doi:10.1016/j.ijrmhm.2014.07.018.

[105] L.S. Sigl, H.F. Fischmeister, On the fracture toughness of cemented carbides, Acta Metall. 36 (1988) 887–897. doi:10.1016/0001-6160(88)90143-5.

[106] A.V. Shatov, S.S. Ponomarev, S.A. Firstov, Hardness and deformation of hardmetals at room temperature, in: V.K. Sarin, D. Mari, L. Llanes, C.E. Nebel (Eds.), Compr. Hard Mater. Vol. 1 Hardmetals, Elsevier Ltd., Oxford, UK, 2014: pp. 345–362. doi:10.1016/B978-0-08-096527-7.00001-5.

[107] H. Engqvist, S. Jacobson, N. Axén, A model for the hardness of cemented carbides, Wear. 252 (2002) 384–393. doi:10.1016/S0043-1648(01)00866-3.

[108] Z.H. Xu, J. Ågren, A modified hardness model for WC-Co cemented carbides, Mater. Sci. Eng. A. 386 (2004) 262–268. doi:10.1016/j.msea.2004.07.061.

[109] S.I. Cha, K.H. Lee, H.J. Ryu, S.H. Hong, Analytical modeling to calculate the hardness of ultra-fine WC-Co cemented carbides, Mater. Sci. Eng. A. 489 (2008) 234–244. doi:10.1016/j.msea.2007.12.036.

[110] A. V. Shatov, S.S. Ponomarev, S.A. Firstov, Modeling the effect of flatter shape of WC crystals on the hardness of WC-Ni cemented carbides, Int. J. Refract. Met. Hard Mater. 27 (2009) 198–212. doi:10.1016/j.ijrmhm.2008.07.008.

[111] T. Csanádi, M. Bľanda, A. Duszová, N.Q. Chinh, P. Szommer, J. Dusza, Deformation characteristics of WC micropillars, J. Eur. Ceram. Soc. 34 (2014) 4099–4103. doi:10.1016/j.jeurceramsoc.2014.05.045.

[112] T. Klünsner, S. Wurster, P. Supancic, R. Ebner, M. Jenko, J. Glätzle, A. Püschel, R. Pippan, Effect of specimen size on the tensile strength of WC–Co hard metal, Acta Mater. 59 (2011) 4244–4252. doi:10.1016/j.actamat.2011.03.049.

[113] J.J. Roa, E. Jimenez-Pique, C. Verge, J.M. Tarragó, A. Mateo, J. Fair, L. Llanes, Intrinsic hardness of constitutive phases in WC-Co composites: nanoindentation testing, statistical analysis, WC crystal orientation effects and flow stress for the constrained metallic binder, J. Eur. Ceram. Soc. (2015) 3419–25. doi:10.1016/j.jeurceramsoc.2015.04.021.

[114] J.M. Tarragó, J.J. Roa, E. Jiménez-Piqué, E. Keown, J. Fair, L. Llanes, Mechanical deformation of WC–Co composite micropillars under uniaxial compression, Int. J. Refract. Met. Hard Mater. 54

(2016) 70–74. doi:10.1016/j.ijrmhm.2015.07.015.

[115] J.J. Roa, P. Sudharshan Phani, W.C. Oliver, L. Llanes, Mapping of mechanical properties at microstructural length scale in WC-Co cemented carbides: Assessment of hardness and elastic modulus by means of high speed massive nanoindentation and statistical analysis, Int. J. Refract. Met. Hard Mater. 75 (2018) 211–217. doi:10.1016/j.ijrmhm.2018.04.019.

[116] P.R. Howie, S. Korte, W.J. Clegg, Fracture modes in micropillar compression of brittle crystals, J. Mater. Res. 27 (2012) 141–151. doi:10.1557/jmr.2011.256.

[117] C.M. Byer, B. Li, B. Cao, K.T. Ramesh, Microcompression of single-crystal magnesium, Scr. Mater. 62 (2010) 536–539. doi:10.1016/j.scriptamat.2009.12.017.

[118] E. Lilleodden, Microcompression study of Mg (0 0 0 1) single crystal, Scr. Mater. 62 (2010) 532–535. doi:10.1016/j.scriptamat.2009.12.048.

[119] D.R.P. Singh, N. Chawla, G. Tang, Y.L. Shen, Micropillar compression of Al/SiC nanolaminates, Acta Mater. 58 (2010) 6628–6636. doi:10.1016/j.actamat.2010.08.025.

[120] H.S. Chou, M.C. Liu, S.Y. Kuan, J.C. Huang, Mechanical behavior of Zr-based and Ta-based micropillars, Intermetallics. 21 (2012) 26–30. doi:10.1016/j.intermet.2011.10.004.

[121] D. Kiener, C. Motz, G. Dehm, Micro-compression testing: A critical discussion of experimental constraints, Mater. Sci. Eng. A. 505 (2009) 79–87. doi:10.1016/j.msea.2009.01.005.

[122] N.A. Fleck, G.M. Muller, M.F. Ashby, J.W. Hutchinson, Strain gradient plasticity: Theory and experiment, Acta Metall. Mater. 42 (1994) 475–487. doi:10.1016/0956-7151(94)90502-9.

[123] E. Camposilvan, M. Anglada, Size and plasticity effects in zirconia micropillars compression, Acta Mater. 103 (2016) 882–892. doi:10.1016/j.actamat.2015.10.047.

[124] A.T. Jennings, M.J. Burek, J.R. Greer, Microstructure versus Size: Mechanical properties of electroplated single crystalline Cu nanopillars, Phys. Rev. Lett. 104 (2010) 1–4. doi:10.1103/physrevlett.104.135503.

[125] D.E. Hurtado, M. Ortiz, Surface effects and the size-dependent hardening and strengthening of nickel micropillars, J. Mech. Phys. Solids. 60 (2012) 1432–1446. doi:10.1016/j.jmps.2012.04.009.

[126] J.R. Greer, W.C. Oliver, W.D. Nix, Size dependence of mechanical properties of gold at the micron scale in the absence of strain gradients, Acta Mater. 53 (2005) 1821–1830. doi:10.1016/j.actamat.2004.12.031.

[127] G. Oncins, J.J. Roa, E. Rayón, J. Díaz, M. Morales, M. Segarra, F. Sanz, Friction, hardness and elastic modulus determined by AFM-FS and nanoindentation techniques for advanced ceramics materials, in: Recent Adv. Ceram. Mater. Res., Nova Science Publishers, Inc., 2013: pp. 215–249.

[128] A.C. Fischer-Cripps, Nanoindentation, Springer Science & Business Media, New York, 2013.

[129] J.M. Antunes, a. Cavaleiro, L.F. Menezes, M.I. Simões, J. V. Fernandes, Ultra-microhardness testing procedure with Vickers indenter, Surf. Coatings Technol. 149 (2002) 27–35. doi:10.1016/S0257-8972(01)01413-X.

[130] W.D. Nix, H. Gao, Indentation size effects in crystalline materials: A law for strain gradient plasticity, J. Mech. Phys. Solids. 46 (1998) 411–425. doi:10.1016/S0022-5096(97)00086-0.

[131] G. Constantinides, K.S.R. Chandran, F. Ulm, K.J. Van Vliet, Grid indentation analysis of composite microstructure and mechanics : Principles and validation, Mater. Sci. Eng. A. 430 (2006) 189–202. doi:10.1016/j.msea.2006.05.125.

[132] ASTM International, ASTM E3-01: Standard practice for preparation of metallographic specimens, (2001). doi:10.1520/E0003-01.

[133] R. Mehta, Interactions, imaging and spectra in SEM, in: Scan. Electron Microsc., 2012: pp. 17–30.

[134] L. Reimer, Scanning Electron Microscopy: Physics of Image and Formation and Microanalysis, 1998.

[135] J. Goldstein, D. Newbury, P. Echlin, J. Alton, D. Roming, C. Lyman, C. Friori, E. Lifshin, Scanning electron microscopy and X-Ray microanalysis: a text for biologists, material scientists, and geologists, Fourth Edi, Springer Science & Business Media, 2012.

[136] A.J. Schwartz, M. Kumar, B.L. Adams, D.P. Field, Electron backscatter diffraction in materials science, Second Edi, Springer, 2009. doi:10.1007/978-0-387-88136-2.

[137] EBSD Oxford Instruments - Introduction to EBSD, (2019). https://nano.oxinst.com/products/ebsd/ (accessed August 22, 2019).

[138] L.A. Giannuzzi, Introduction to focused ion beams: instrumentation, theory, techniques and practice, Springer Science & Business Media, 2006.

[139] H. Fei, A. Abraham, N. Chawla, H. Jiang, Evaluation of micro-pillar compression tests for accurate determination of elastic-plastic constitutive relations, J. Appl. Mech. 79 (2012) 061011 1–9. doi:10.1115/1.4006767.

[140] H.G. Jones, A.P. Day, D.C. Cox, Electron backscatter diffraction studies of focused ion beam induced phase transformation in cobalt, Mater. Charact. 120 (2016) 210–219. doi:10.1016/j.matchar.2016.09.004.

[141] D.B. Williams, C.B. Carter, Transmission electron microscopy : a textbook for materials science, 2nd ed., Springer US, 2009. doi:10.1007/978-0-387-76501-3.

[142] L. Reimer, H. (Helmut) Kohl, Transmission electron microscopy : physics of image formation, 5th ed., Springer-Verlag New York, New York, 2008. doi:10.1007/978-0-387-40093-8.

[143] B. Poon, D. Rittel, G. Ravichandran, An analysis of nanoindentation in linearly elastic solids, Int. J. Solids Struct. 45 (2008) 6018–6033. doi:10.1016/j.ijsolstr.2008.07.021.

[144] C.A. Volkert, E.T. Lilleodden, Size effects in the deformation of sub-micron Au columns, Philos. Mag. 86 (2006) 5567–5579. doi:10.1080/14786430600567739.

[145] W.C. Oliver, G.M. Pharr, An improved technique for determining hardness and elastic modulus using load and displacement sensing indentation experiments, J. Mater. Res. 7 (1992) 1564–1583. doi:10.1557/jmr.1992.1564.

[146] J.M. Tarragó, S. Dorvlo, J. Esteve, L. Llanes, Influence of the microstructure on the thermal shock behavior of cemented carbides, Ceram. Int. 42 (2016) 12701–12708. doi:10.1016/j.ceramint.2016.05.024.

[147] M.D. Uchic, D.M. Dimiduk, A methodology to investigate size scale effects in crystalline plasticity using uniaxial compression testing, Mater. Sci. Eng. A. 400–401 (2005) 268–278. doi:10.1016/j.msea.2005.03.082.

[148] C. Verge, Efecto de la orientación cristalina en la dureza del carburo de wolframio, BSc. thesis, Universitat Politècnica de Catalunya, 2014.

[149] F. Ulm, M. Vandamme, C. Bobko, J.A. Ortega, Statistical indentation techniques for hydrated nanocomposites: concrete, bone, and shale, J. Am. Ceram. Soc. 9 (2007) 3677–2692. doi:10.1111/j.1551-2916.2007.02012.x.

[150] G. Constantinides, F. Ulm, K. Van Vliet, On the use of nanoindentation for cementitious materials, Mater. Struct. 36 (2003) 191–196. doi:10.1007/bf02479557.

[151] J.J. Roa, E. Jiménez-Piqué, J.M. Tarragó, M. Zivcec, C. Broeckmann, L. Llanes, Berkovich nanoindentation and deformation mechanisms in a hardmetal binder-like cobalt alloy, Mater. Sci. Eng. A. 621 (2015) 128–132. doi:10.1016/j.msea.2014.10.064.

[152] H. Doi, Y. Fujiwara, K. Miyake, Mechanism of plastic deformation and dislocation damping of cemented carbides, Trans. Metall. Soc. AIME. (1969) 1457–70.

[153] A.M. Korsunsky, M.R. McGurk, S.J. Bull, T.F. Page, On the hardness of coated systems, Surf. Coatings Technol. 99 (1998) 171–183. doi:10.1016/S0257-8972(97)00522-7.

Chapter 4

Scientific publications

4 Scientific publications

The present study is divided in two parts. The first one corresponds to the evaluation of the possible size effect on the mechanical properties and behavior of cemented carbides due to microscale testing (Articles I and II). The second one addresses the role of both WC and binder on the mechanical response at small length scales of hardmetals, by studying composited with partial and total substitution of Co as binder and WC as hard phase (Articles III and IV). In addition, a validation of the testing protocols was done by linking strain phenomena from uniaxial compression of micropillars with flow stress of the constrained Co binder from analysis of data obtained by massive nanoindentation testing (Article III).

Following the above structure, scientific publications are presented next.

Article I - Scale effect in mechanical characterization of WC-Co composites

D.A. Sandoval, A. Rinaldi, J.M. Tarragó, J.J. Roa, J. Fair, L. Llanes. Int. J. Refract. Metals Hard Mater. 72 (2018) 157-162.

Uniaxial compression of micropillars is a technique widely used for evaluation of mechanical properties of metallic and ceramic materials. However, its implementation for studying composite materials is quite recent. For pure metals and metallic alloys, the effect on the specimen size is well understood - on the basis of a Hall-Petch relationship. This first article addresses the size effect issue on the mechanical response of WC-Co cemented carbides by means of uniaxial compression of micropillars. In doing so, micropillars of different diameters were milled on one medium-grained WC-Co sample, with d_{pillar}/d_{WC} ratios ranging from 4 to 1. Aspect ratio and taper angles were kept similar on all micropillars. A clear evidence of size effect was found: the smallest micropillar showed deformation/failure mechanisms observed for WC alone. For bigger sample sizes, the mechanical response involved several mechanisms such as plastic flow of Co binder, deformation of Co and WC and phenomena at WC/WC and WC/Co interfaces, associated with the composite nature of the bulk material.

Article II - Influence of specimen size and microstructure on uniaxial compression of WC-Co micropillars

D.A. Sandoval, A. Rinaldi, A. Notargiacomo, O. Ther, E. Tarrés, J.J. Roa, L. Llanes. Ceram. Int. 45 (2019) 15934-15941 .

The matter of size effect and its influence on the mechanical response of cemented carbides is deepened in this study. Micropillars of 2 μm in diameter milled in three WC-Co grades with fine, medium and coarse carbide grain size were investigated (d_{pillar}/d_{WC} ratios of 5, 2 and 1, respectively). First, evaluation and selection of a representative elementary volume (REV) – based on volume fractions of constitutive phases – was done, to consider each sample as a bulk. Experimental findings indicate that volume fraction of phases within micropillars should be at least 85% that of the bulk, to overcome the size effect issue. By selecting the correct sample size, elastic modulus estimated from load-displacement curves, was within the range expected for WC-Co with similar volume fractions of binder. The relationship between microstructure and mechanical response was evidenced as strain bursts in σ-ε, associated with deformation/damage features observed in the micropillars after uniaxial compression.

Article III - Micromechanical properties of WC-(W,Ti,Ta,Nb)C-Co composites

D.A. Sandoval, J.J. Roa, O. Ther, E. Tarrés, L. Llanes. J. Alloys Compd. 777 (2019) 593-601.

Hardness of constitutive phases of a complex cemented carbide was evaluated by means of massive nanoindentation. The methodology followed allowed to evaluate intrinsic hardness of WC (and its dependence on the crystallographic orientation, i.e. basal and prismatic planes), the mixed cubic carbide (W,Ti,Ta,Nb)C, and the constrained Co binder. Results showed that the mixed cubic carbide is significantly harder than WC, regardless the hardness anisotropy exhibited by the later. By further deconvolution of data gathered for Co binder – using thin film models - it was found that hardness and flow stress of the metallic binder are strongly influenced by the hardness of the substrate, i.e. carbide particles. Effective flow stress of the constrained metallic binder was estimated with the attained hardness values and validated by correlating it with strain bursts occurring at different stress and strain levels, as discerned in σ-ε curves determined from uniaxial compression testing of micropillars.

Article IV - WC-base cemented carbides with partial and total substitution of Co as binder: Evaluation of mechanical response by means of uniaxial compression of micropillars

D.A. Sandoval, A. Rinaldi, A. Notargiacomo, O. Ther, J.J. Roa, L. Llanes. Int. J. Refract. Metals Hard Mater. 84 (2019) 105027.

Uniaxial compression of micropillars was used to induce plastic deformation and damage in micropillars milled in WC-Co, WC-CoNi and WC-NiMo cemented carbides, with similar binder content and microstructural parameters. After testing, yielding events discerned in σ-ε curves, pointed out that plastic deformation at initial loading is intrinsic to the chemical nature of the binder. In this sense, deformation and plastic flow of binder was strongly dependent on binder free surfaces within the micropillar, and by constraining effect of the surrounding WC particles. Furthermore, yielding phenomena and strain hardening was higher for NiMo and lower for CoNi binders, compared to Co one. TEM inspection indicated different main plastic deformation mechanisms as function of chemical nature of the binder: fcc to hcp transformation for Co; fcc to hcp transformation with dislocation-mediated activity for CoNi; and dislocation activity for NiMo. Yield stress related to glide at WC/WC differed for the three materials, although sliding resistance at carbide interface were found to be alike for all of them.

Chapter 5

Summary of results

5 Summary of results

In this PhD thesis, systematic testing protocols to evaluate the micromechanical behavior of cemented carbides have been proposed and implemented. They focused on the assessment of the intrinsic properties and response of the constitutive phases of these materials. The thesis followed a structure in which reliability of the testing protocols was first evaluated based on size effects linked to small scale testing. A minimum representative elementary volume (REV) was found suitable to obtain reproducible results. Then, findings obtained by uniaxial compression of micropillars were compared with those determined through nanoindentation testing, regarding local properties of the constrained binder. Finally, micromechanical response of cemented carbides with partial substitution of WC as well as partial or total substitution of Co was evaluated and compared to that of WC-Co.

5.1. Evaluation of the size effect on mechanical characterization of cemented carbides at small length scale

Size effect issue was approached by two perspectives. The first one regarding the ratio between micropillar diameter and carbide mean grain size ($d_{pillar}/d_{carbide}$). The second one, concerning the volume fraction of phases contained in one micropillar.

As it could be expected, the size of the sample influences the overall mechanical response of the micropillar. In this sense, as $d_{pillar}/d_{carbide}$ ratio is lower than 1, i.e. the diameter of the micropillar is within the range of or smaller than the mean carbide grain size, the response observed is that of the carbide phase. Furthermore, plastic deformation of WC depends on its orientation with respect to the compressive load. In addition, higher stiffness values than those expected for the composite are needed to induce an elasto-plastic behavior. On the other hand, as $d_{pillar}/d_{carbide}$ ratio gets around 2, the mechanical response of the micropillar emulates that of the bulk material in terms of elastic behavior.

Regarding plastic deformation, stress-strain curves suggest that observed phenomena after compression are a combination of intrinsic response of each constitutive phase of the material (metallic binder and carbides), the constraint degree of the binder by the surrounding carbide particles, and the orientation and disposition of phases within the micropillar.

From the representative elementary volume (REV) perspective, the volume fraction of constitutive phases within the micropillars was compared to that of the bulk. To overcome the size effect issue, it was found that the volume fraction of both binder and carbide phases in the former should differ less than 15% from those in the later.

The size effect issue in uniaxial compression of micropillars of cemented carbides can be avoided with a proper selection of a sample size, in terms of micropillar dimensions, microstructural length scale of the bulk material, and volume fraction of constitutive phases. In this PhD thesis, such condition was found to be satisfied for micropillars with $d_{pillar}/d_{carbide}$ ratio of 2, containing volume fraction of phases within the micropillar no more than 15% different from those determined in the bulk material. It allowed to get both an elastic response comparable to that of the bulk and reproducible results in the elasto-plastic behavior of the tested micropillars. Using specimens with appropriated dimensions yielded elastic modulus was 430 ± 47 GPa and 625 ± 103 GPa for medium- and fine-grained grades respectively, within the range of the values expected for a WC-Co cemented carbide with comparable volume fraction of binder.

Finally, constraining effect of the surrounding carbide particles was evidenced on the loading curves as pop-in events. Such strain bursts were found at higher stress levels for the fine grade than for the medium one, in agreement with the lower effective ductility expected from a more constrained binder in the former than in the later.

5.2. Mechanical response of cemented carbides with partial and total substitution of Co and partial substitution of WC, by means of small-scale testing

The issue of criticality of WC and Co as primary raw materials for cemented carbides is a major motivation for this PhD thesis. Therefore, intrinsic mechanical properties and response of constitutive phases were evaluated for one cemented carbide with partial substitution of WC and other two with partial and total substitution of Co as binder.

Implementation of massive nanoindentation and statistical analysis of the gathered data allowed to validate the anisotropic character of the intrinsic hardness for WC: around 19 and 25 GPa for prismatic and basal planes respectively, in fair agreement with values found in the literature. It was different from the isotropic behavior discerned, as expected, for the intrinsic hardness of the mixed cubic carbide (W,Ti,Ta,Nb)C. However, variations from 23 to 38 GPa were found in this cubic phase, possibly associated with nonstoichiometric nature and/or heterogeneity in chemical composition of the carbide.

Intrinsic hardness for the Co binder was determined to be around 6 GPa, after consideration of the constraining effect of the surrounding carbide particles. Such value is 36% lower than the one found directly from nanoindentation testing. Furthermore, it was found that constraining of the metallic binder imposed by the ceramic phase also affects its flow stress, ranging from 1.3 to 2 GPa depending on the carbide particles surrounding it.

Plastic deformation phenomena occurring in WC and binders with different chemical nature were evaluated for WC-Co, WC-CoNi and WC-NiMo grades. Results showed that plastic deformation of the binder phase differs depending upon its chemical nature. In this sense, Co binder exhibited hcp laths preferentially, as a direct consequence of the stress-induced fcc to hcp martensitic transformation. By substituting Co by Ni, the later mechanisms shifted towards planar slip. Dislocations arrays were heterogeneously observed within binder regions, possibly due to an inhomogeneous distribution of stresses and strains because differences in stiffness of the constitutive phases as well as variable geometry within phase assemblage of the composite.

Constraining of metallic binder – together with intrinsic ductility of the metallic binder alloy – was evidenced as pop-in events in the stress-strain curves. They emerged at different stress/strain levels for micropillars milled in the same cemented carbide grade. However, resistance at WC/WC boundaries was estimated (around 2 GPa) to be independent of the chemical nature of the binder.

Understanding the mechanical behavior of each constitutive phase of cemented carbides is a key factor for tailoring new alloys on the basis of microstructural design. In doing so, two testing protocols at micro- and nanometric length scales were systematically followed to evaluate such intrinsic behavior and its effect on the overall response of cemented carbides. On one hand, massive nanoindentation and the analysis of statistical data through methods proposed for composite materials, was a validated as a successful approach to determine the intrinsic hardness of constitutive phases in a simple binder-carbide structure, as well as in a more complicated one, composed by two carbides of different chemical nature. Furthermore, flow stress of binder was extracted from hardness values obtained from massive nanoindentation, and further treatment of data by thin film models (e.g. by using the Korsunsky and/or Puchi-Cabrera models). On the other hand, uniaxial compression of micropillars allowed to link plastic flow of the binder – determined from analysis of data gathered from massive nanoindentation testing – with strain bursts found in the stress-strain curve extracted from the loading-unloading cycle.

Flow stress for the constrained metallic binder was estimated to be between 1.3 and 2.0 GPa. Those values were in satisfactory agreement with the stress levels at which pop-in events were later observed on stress-strain curves from uniaxial compression of micropillars. Higher and lower bounds should be linked to plastic flow of highly constrained and unconstrained metallic binder respectively. It sustains the reliable estimation of flow stress for the constrained metallic binder from the intrinsic hardness value evaluated from statistical analysis of the data attained through massive nanoindentation testing.

Chapter 6

General conclusions and perspectives

6 General conclusions and perspectives

6.1 General conclusions

In this PhD thesis, uniaxial compression of micropillars and massive nanoindentation were selected to evaluate the mechanical response of cemented carbides at small length scales, with the aim of understanding the role played by each phase in the overall mechanical response of the composite material. Based on the research carried and the results obtained, the following conclusions may be drawn:

1. Mechanical response of cemented carbides evaluated by uniaxial compression of micropillars is size-affected. In this sense, for a sample size approaching the WC mean grain size, the mechanical behavior is that of the carbide phase. On the other hand, as the sample size gets bigger, the mechanical response is a combination of deformation and failure mechanisms of the constitutive phases which approaches to that of the bulk material.

2. To overcome the size effect issue, an appropriate selection of the sample size - considering the ratio between the micropillar diameter and the mean carbide grain size – should be done. In this work it was found that an appropriate test specimen is obtained when the difference between the volume fraction of constitutive elements within micropillars and that of the bulk material is less than 15%.

3. Uniaxial compression testing protocol followed in this work with imposed maximum load and displacement around 20 mN and 300 nm, respectively, allowed to obtain reproducible results regarding measured mean value and dispersion for elastic modulus. It was concluded after testing a population of micropillars milled on fine- and medium-grained grades of cemented carbides that met the size conditions referred above.

4. Constraining effect imposed by the carbide particles on the metallic binder is evidenced in the loading part of stress-strain curves as strain-bursts linked to deformation and damage features observed on the compressed micropillars. They occur at stress levels which are proportional to the effective constraining degree of the metallic binder. Furthermore, the stress values at which local plasticity events are discerned agree with the flow stress ones estimated from hardness values obtained by means of massive nanoindentation; thus, the former may be considered as experimental validation of the latter.

5. Implementation of statistical analysis of massive nanoindentation data, allows to determine intrinsic hardness of constitutive phases of complex composites with more than one carbide phase. Furthermore, it allows to discern the isotropy/anisotropy character in hardness of them (e.g. anisotropic for WC, where basal orientation is around 30% harder than prismatic one).

6. Assessment of intrinsic hardness of the constrained metallic phase - determined by data analysis from massive nanoindentation testing – requires further analysis based on thin film models. Within this regard, substrate influence on hardness values decreases as effective constraining of the ceramic particles on the metallic phase increases.

7. Plastic activity at early stages of loading in uniaxial compression of micropillars corresponds to that of the binder, which is intrinsic to its chemical nature. In this sense, higher yield stresses and strain hardening rates (SHR) were found for NiMo binder. On the other hand, lowest values were found for the cemented carbide with partial substitution of Co by Ni.

8. Frequency and stress/strain levels at which strain bursts occurred are dependent on the intrinsic ductility of the binder phase (through phase transformation, slip activation and/or dislocation activity), as well as on constraint degree imposed by surrounding carbide particles.

9. Gliding of carbides at WC/WC interfaces was evidenced in stress-strain curves as a plateau-like yielding event. Distribution of particles and orientation with respect to the applied load affect strongly the stress levels at which the former event occurs. Nevertheless, WC/WC glide resistance was similar (around 2GPa) for WC-Co, WC-CoNi and WC-NiMo.

10. Plastic deformation mechanisms within binder change from fcc-hcp transformation to dislocation-mediated activity as Co is substituted by Ni. For NiMo, dislocation density is affected by the amount of Mo in the alloy. Such effect was evidenced in stress-strain curves as a pronounced strengthening.

6.2 Perspectives

Nowadays the awareness on difficulties to obtain raw materials, together with their impact on the environment and most important, the human health, have led research to search and find other materials that can replace those considered critical. This issue is also an important reason for promoting research

on the hard materials community. In this PhD thesis it was considered the study of the mechanical response of cemented carbides at local length scales as the baseline to understand the role of each phase – hard carbide and soft metallic one – in the overall behavior of the composite material. Main goal behind it was to design new compositions with substitution of critical raw materials. Within this context, the major findings of this work were the development of a testing protocol to evaluate mechanical properties at small length scales, such as hardness and elastic modulus, and mechanical response, such as plastic deformation phenomena intrinsic of each constitutive phase, for cemented carbides.

Furthermore, it was understood the effect of the constraining effect of the carbide particles on the metallic binder, which changes its elastic and plastic response at local scale. In this regard, testing protocols followed in this PhD thesis could be implemented at higher temperatures to evaluate the mechanical properties and response of the material under service-like conditions.

Finally, the knowledge on the local response of constitutive phases gathered in this thesis and in future works, will be the input information for simulation models. It can further improve and accelerate the development of new cemented carbide alloys, designed for specific applications. In this sense, sequential sectioning of micropillars after uniaxial compression would be the next step to simulate all the phenomena occurring during testing in real time. Thus, tailoring of cemented carbides based on their microstructural parameters and the chemical nature of their constitutive phases, targeting a specific application, will become a less difficult and more effective task.

Acknowledgements

Official acknowledgments of institutions are included at the end of each scientific paper. The following words are for those who were with me side by side during some part or my whole PhD thesis.

In many PhD thesis I have read that this is the harder chapter to write. In my opinion this is only true if one is so stressed that a person can be forgotten. This could be my case, so I apologize in advance if I forget to mention anyone. However, this is only a way to keep documented how grateful I am to all of you who have being walking with me this road. But I'm sure you all know who you are because I've tried to let you know with a smile, a gesture, a "thanks", that your support has being important to help me achieve this goal.

First, I would like to thank my supervisor Luis Llanes. I remember when I went for the first time to his office to ask him for a possible Master Final Project. At that moment I was studying the AMASE program. I remember, I called him "professor" (as an unreachable figure), as it is common in Venezuela. With time I got to see the wonderful and friendly person he is, so that figure of "professor" became just Luis. To Luis I thank not only that he had a Master Final Project for me, but a PhD opportunity for which he thought I was suitable. But this was much more than that, this was the opportunity for me to stay in Europe and "scape" the situation in my country which was getting worse (and continues to). This was an opportunity to change my life and being in the road to achieve so many things that I could not even think to achieve if I stayed in Venezuela. For changing the path of my life (and of those around me), I'm so grateful Luis. I also thank you for teaching me so many things. You taught me all (that time allowed) about hard materials (even though somethings had nothing to do with my thesis), how to approach to technical issues, how to manage resources efficiently, how to work in a team, to be politically correct, to empathize with others, to think always in a solution before approaching to someone with a problem. This list goes on and on. For helping me to be a better professional and a better person I'll always be grateful to you.

I also would like to thank to Joan Josep to introduce me the wonderful micromechanical testing world. In which with a tiny sample, a lot of tests could be done. Thank you for all the knowledge you shared with me in this not so common matter for cemented carbides, and for your support with all the testing in and outside UPC.

To CIEFMA group, all the professors and students who were there supporting my work, even when they didn't notice it. Specially to Emilio, for breaking down his barriers and sharing with me important moments of my journey like at Plansee Seminar, where he was my guide to all the people I was meeting

(and also to buy a fridge magnet and *gorduritas*); and in Thailand, where he trusted me to be his right hand with all the work we had to do. Also, for helping me to overcome the fear of talking for the first time in an international conference. You have been a very important person in my professional growth.

A great part of my work was done with the help of Dr. Antonio Rinaldi at ENEA (Italy). Antonio, I'm so grateful you have taken the time not only to receive me in Italy and ENEA, but also to stay with me so late compressing the micropillars, to discuss with me all the results, to read the papers, etc. I also thank you for making me feel at home while working at ENEA. You are a very good friend and I appreciate your willingness and honesty at all times.

To Federica and Eloisa who were my colleagues at ENEA, thanks for helping me with everything, from transportation to how the lunch menu worked, to how to print something. For taking me to have l'aperitivo and for showing me around the beautiful Rome. Thanks to Dr. Andrea Notargiacomo for helping me with milling micropillars at such short notice and all his explanations about the FIB. Thanks also to COST Action "Critical Raw Materials Under Extreme Conditions" for granting me the scholarships with which I went to Italy. Without this opportunity I would not have met such wonderful people.

Thanks to the R&D team of Hyperion Materials & Technologies for supporting me in every conference and for listening my presentations of a subject very far from their daily work. Special thanks to Olivier Ther and Elena Tarrés for their help in analyzing results and very careful revisions of publications that always helped me to improve them.

At UPC I have to thank so many people. At the top of the list is Dr. Trifon Trifonov (Traifon Traifonov with affection), not only for the many hours he/we spent in front of the SEM milling micropillars, lamellae, taking images, but also for the good and bad jokes (that always ended in good laughter), for the many stories we told, for the bad (or good) music he had me listening, for the great videos of him and his friends skydiving, for the time we spent "*revisando las instalaciones*" in which we relaxed after being hours working in that freezing microscopy room. Thank you Dr. TT, heavy metal is still alive! To Fernando for receiving me in CIEFMA's labs at the very beginning of my work. To Isaac to spend also so many hours trying to find nanoindentations in cemented carbides (a needle in a haystack), and a critical defect in a very fine microstructure (again, the needle). I also would like to thank all the students that directly or not helped me with my work. Specially Sandra and Saloua who helped me with so many tests and sample preparation. To Chloe and Rita because thanks to them I knew other topics related to cemented carbides. And, although not directly related to my PhD, to Marc because come on, you are simply the best!

Now it is your turn pollitos! I love you so much that I wanted you to suffer reading all the acknowledgements before you find yourselves. Where to start with you? First, I would like to thank José María because he was the very first person to teach me how things worked around CIEFMA. I remember he told me "don't worry, with your personality you'll do well here", so that gave me a lot of confidence (a lot!). Thanks to Quentin for making me laugh so much at the office and for being my partner in crime whit the *alcachofa* code word. To Dani because when she (finally) decided to join the group I was able to speak in "venezuelan". Finally, I had someone who understood (almost) everything I said at once! Thank you, Dani, because being who I am with all my Venezuelan stuff have helped me so much through these years. You understand me very well and I'm happy to have you to share so many aspects of my life. To Miquel (for reference Dr. Miguel Turón-Vinyasa), for all those coffee hours talking about everything and nothing at the same time, for helping me with my lack of creativity, for making me laugh so much, for teaching me about investments, and for translating the abstract to Catalan. To Erica for sharing with me her way of seeing life, especially when chasing the guy with the best *arroz con leche* in Spain. To Mireia for helping me to acknowledge the richness of culture and landscapes of Catalunya, and to Roberta, for being an example of strength when I was going through rough times. To you *hermano* (Giuseppe) for sharing all your brightness and greatness with me, and for letting me speak for few minutes in all the time we have being knowing each other. Thank you, Rom, also for the great laughs, I'm sorry we made you our target sometimes, but you have no idea how many of those times I was having a rough day and you made me forget about everything just with your great attitude! To Yass for being there when I needed him, even though you were so busy at that time that you were barely a living person. To Jing for teaching me how to smile politely to avoid awkward questions. To Bernie for brighten up our days while you were here. And finally, to Erik for all the craziness you add to every pollito's meeting. And to all of you for introducing me to Andrés, Inma, Mel, Carmen, Jero and Cecile who are the best "extension" of this group. I'm so grateful for being part of this amazing gang.

I also want to thank Daniel. Some people say that the times of God are perfect. Well, you came to Barcelona in the perfect time. Thank you so much for encouraging me to write my fourth paper and to share with me a couple of long Saturdays at the library. Without your enthusiasm it would have taken me so long. Thank you so much! And to Irene just for being so crazy that makes Miquel look as a baby in diapers. Thank you for all the good stories and the opportune advices.

I would like to thank also my office mates Anna, Karen, Quim, Marcel, Priya and Elia. You were the best company. Each one of you contributed to have the best office with the perfect balance between working and relaxing time.

Finally, to my family who always give me their love that helps me to continue enjoying what I do. To my husband Iam, who have been all the time at backstage with me, taking all the good and the bad. I simply couldn't have done this without you by my side, your support and admiration in all that I do and accomplish pushes me to continue. I think this is a chapter in our lives we both walked together and now we are closing it together.

In summary,

Gracias... Totales!